



**HAL**  
open science

## Design, performance characterization and applications of continuous oscillatory baffled reactors

Marco Avila, Beatrice Kawas, David Frederick Fletcher, Martine Poux, Catherine Xuereb, Joelle Aubin

### ► To cite this version:

Marco Avila, Beatrice Kawas, David Frederick Fletcher, Martine Poux, Catherine Xuereb, et al.. Design, performance characterization and applications of continuous oscillatory baffled reactors. *Chemical Engineering and Processing: Process Intensification*, 2022, 180, pp.108718. 10.1016/j.cep.2021.108718 . hal-03763541

**HAL Id: hal-03763541**

**<https://hal.science/hal-03763541v1>**

Submitted on 1 Sep 2022

**HAL** is a multi-disciplinary open access archive for the deposit and dissemination of scientific research documents, whether they are published or not. The documents may come from teaching and research institutions in France or abroad, or from public or private research centers.

L'archive ouverte pluridisciplinaire **HAL**, est destinée au dépôt et à la diffusion de documents scientifiques de niveau recherche, publiés ou non, émanant des établissements d'enseignement et de recherche français ou étrangers, des laboratoires publics ou privés.

# Design, performance characterization and applications of continuous oscillatory baffled reactors

Marco Avila<sup>a</sup>, Beatrice Kawas<sup>a</sup>, David Frederick Fletcher<sup>b</sup>, Martine Poux<sup>a</sup>, Catherine Xuereb<sup>a</sup>, Joelle Aubin<sup>a,\*</sup>

<sup>a</sup>Laboratoire de Génie Chimique, Université de Toulouse, CNRS, INPT, UPS, Toulouse, France

<sup>b</sup>School of Chemical and Biomolecular Engineering, The University of Sydney, NSW 2006, Australia

## Abstract

The continuous oscillatory baffled reactor (OBR) is a particular type of tubular reactor, which has drawn increasing attention over the past few decades due to the benefits it provides in terms of intensification of heat and mass transfer, as well as equipment compactness compared with stirred tank reactors. This process enhancement is principally due to the interaction of the oscillatory flow with internal baffles and the consequent generation of transverse flows and eddies. Continuous OBRs are already applied in several industrial sectors, however these reactors present certain limitations in terms of operating conditions and the range of possible applications. This review presents and discusses the current knowledge on continuous OBR design guidelines, performance characterization and applications. It aims to guide the selection of the most appropriate continuous OBR design, as well as the characterization criteria, according to the type of application and final process objective.

**Keywords:** COBR, continuous oscillatory flow, mixing, heat transfer, energy dissipation, multiphase systems.

---

\* Corresponding author at : Laboratoire de Génie Chimique, 4 allée Emile Monso BP-84234, 31432 Toulouse Cedex 4, France. Tel.: +33 5 34 32 37 14 ; fax : +331 5 34 36 97  
E-mail address: joelle.aubin@ensiacet.fr (J. Aubin).

## 1 Introduction

The development of green and sustainable technologies is of prime importance for the chemical and process industries due to increasing social and environmental concerns. One of the major challenges that these industries face currently is the creation of innovative processes for the production of commodity and intermediate products that allow high product quality with specified properties and that are less polluting, as well as more efficient in terms of energy, raw materials and water management.

Continuous processing offers many benefits over batch operation, as it minimizes waste (Schaber et al., 2011), reduces energy consumption (Yoshida et al., 2011), improves mass and heat transfer (Singh and Rizvi, 1994; Yu et al., 2012), as well as chemical conversion (Hartman et al., 2011). Nowadays, new technologies and devices, such as static in-line mixers, packed bed reactors, microreactors, heat exchange reactors and oscillatory baffled reactors, have been developed to achieve enhanced transport phenomena with compact designs.

The continuous oscillatory baffled reactor (OBR) is a particular type of tubular reactor, typically equipped with periodically located sharp-edged orifice baffles along its length, as is shown in Figure 1. This type of reactor operates with a periodic oscillatory (or pulsed) flow that is superimposed upon a net flow. The pulsed flow interacts with the baffles, thereby causing effective transverse flows and enhanced transport. It should be pointed out that many of the pioneering studies on oscillatory baffled reactors were performed in batch mode (i.e. with no net flow) and a considerable amount of knowledge from these studies is still employed today for the design of continuous OBRs. This is generally considered a valid approach, as the oscillatory flow typically dominates the net flow rate in continuous OBRs.

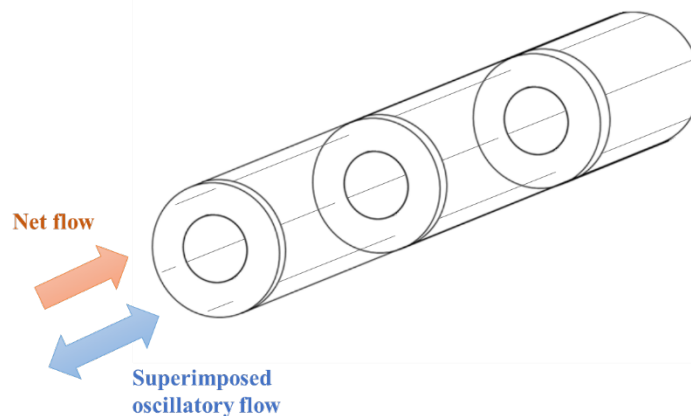


Figure 1: Schematic diagram of a continuous oscillatory baffled reactor with single orifice plate baffles.

Due to the interaction of fluid pulsations with the baffles and the resulting recirculating flow, mixing performance in continuous OBRs is independent of the net flow, thereby providing good mixing quality and long residence times (comparable with those obtained in batch reactors) in a compact geometry with a greatly reduced length-to-diameter ratio tube (Harvey et al., 2003). Due to these characteristics, COBRs have proven to intensify processes globally, leading to operations that use less energy and produce less waste compared with processes in conventional STRs (Phan et al., 2011a; Reis et al., 2006b).

The literature on continuous OBRs is relatively abundant and studies range from general performance characterization, such as residence time distributions (RTD) and mixing, to examples of process intensification for specific applications. There are also a number of review articles that focus on some specific aspects, such as applications of oscillatory flow (Ni et al., 2003b), biofuel production (Masngut et al., 2010), biological processes (Abbott et al., 2013), mesoscale OBRs (McDonough et al., 2015), crystallization (McGlone et al., 2015) and synthetic chemistry applications (Bianchi et al., 2020).

Whilst the current literature on OBRs appears diverse and varied, it is also apparent that most studies employ the single orifice baffle geometry; other internals such as helical baffles, multi-orifice plates and the disc-and-doughnut baffle, which have proven efficiency for multiphase flow in extraction columns, have been studied very little. As a result, most of the recommended design guidelines of OBRs have been obtained for the single orifice baffle geometry, however these design rules may not be strictly applicable to all other geometries. Moreover, the existing design guidelines for OBRs have been established for a specific range of operating or flow conditions, a specific performance characteristic (typically RTD) and most often for single phase flow. However, these design rules appear to be used in the literature without limits for any system, whether it be single or multiphase flow, and for any operating and flow conditions. Indeed, it is far from certain that the current design rules are well adapted to all situations.

This article reviews the current literature in terms of design guidelines for continuous OBR geometries, flow performance characterisation and applications. It aims to identify the limitations of the current recommended operating conditions and design guidelines, and to outline the importance of the choice of performance characterisation method with respect to the process objective.

## **2 Flow and reactor design**

The overall mechanism of eddy formation in OBRs has been described widely in the literature (Brunold et al., 1989; Gough et al., 1997; Mazubert et al., 2016a; McDonough et al., 2015; Ni et al., 2002). Typical flow patterns formed in continuous OBRs with orifice baffles are shown in Figure 2. During the flow acceleration phase (Figure 2(a)), eddies are formed downstream of the baffles and flow separation starts. As the oscillatory velocity increases (Figure 2(b)), the eddies start to fill the baffle cavity. At the flow reversal phase (Figure 2(c)), the eddies are detached from the baffle, leaving a free vortex that is engulfed by the bulk flow and that interacts with other vortices that were generated in previous cycles (Figure 2(d)), before restarting the cycle again.

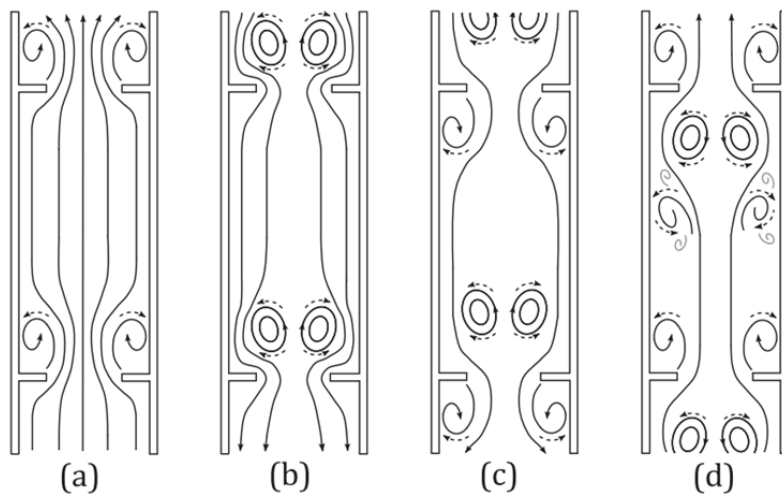


Figure 2: Eddy formation in a continuous oscillatory baffled reactor (McDonough et al., 2015).

## 2.1 OBR geometry

### 2.1.1 Baffle designs

Sharp-edged single orifice baffles (as shown in Figure 1) are the most common baffle design used in OBR studies, however there are a number of other baffle geometries that have been studied in the literature. These geometries are shown in Table 1 and include periodic smooth constrictions, multi-orifice plates, disc-and-doughnuts, various helical forms (e.g., round wires, sharp-edged and alternating ribbon, double ribbons, combined with a central rod), central disc baffles, and wire wool.

Periodic smooth constrictions are based on the single orifice plate baffle design. The main difference is that the orifices in smooth constriction baffles are made by constricting the reactor tube (usually made with glass). This design has been shown to provide effective radial mixing, which is equivalent to that achieved with single orifice baffles (Reis et al. (2005)). However, compared with

orifice plate baffles, these smooth constrictions offer low and uniform shear rates, which may be advantageous for applications such as shear-sensitive bioprocesses (Reis et al., 2006a, 2006b).

Multi-orifice plates used in OBRs are the same as those in the pulsed and reciprocating multi-orifice plate columns for liquid-liquid extraction applications. This geometry is attractive due to the ease of manufacture. The influence of the number of orifices on the performance of the OBR was studied by González-Juárez et al. (2017). A higher number of orifices was found to reduce dead zones and enhance radial mixing due to the generation of a larger number of smaller eddies. The hydrodynamic performance of multi-orifice plate OBRs is related to the effective tube diameter,  $D_e = \sqrt{D/n}$  (Smith (1999)). As  $D_e$  decreases, the RTD curves become narrower with a more uniform concentration in the cross-section, thus improving the plug flow behaviour and the mixing quality. Ahmed et al. (2018b) studied mass transfer in air-water systems for different OBR geometries and concluded that the multi-orifice design is recommended over the smooth constrictions, single orifice and helical baffle geometries for gas-liquid mass transfer applications. Indeed, the multi-orifice geometry offers better control of the size and shape of the bubbles, offering a wider bubbly flow region and higher volumetric mass transfer coefficient than the other geometries. One type of multi-orifice baffle is the tri-orifice design with central rod. This geometry has proven to be successful for the transesterification of vegetable oils, which is a mass transfer limited liquid-liquid reaction that benefits from the generation of small droplets due to the high shear rates produced at the orifices (Soufi et al., 2017).

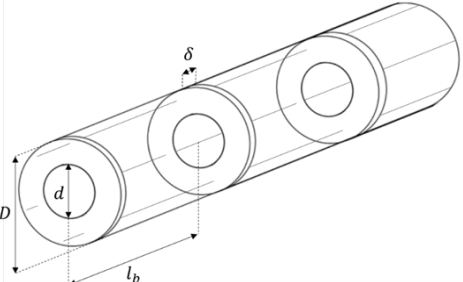
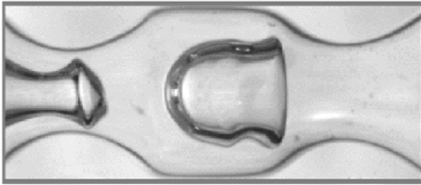
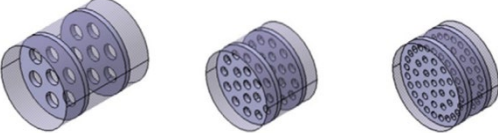
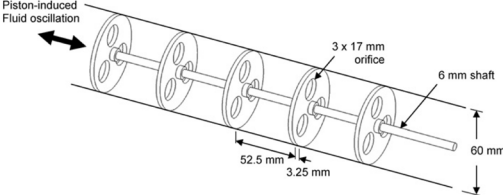
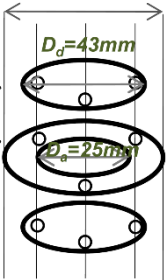
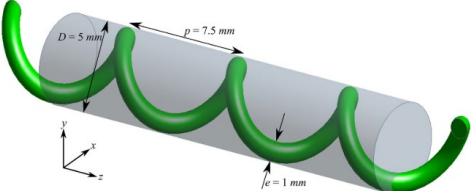
In the disc-and-doughnut geometry, the disc placed between the orifice plates acts as a barrier to the dominant axial flow in the centre of the tube, and thereby generates additional radial flow. This design has also been used in liquid-liquid extraction columns for a long time (Al-Khani et al., 1988; Angelov et al., 1990; Laulan, 1980; Leroy, 1991; Martin, 1987) and also for emulsion polymerization (Lobry et al., 2013). Mazubert et al. (2016a, 2016b) studied the hydrodynamics generated by the disc-and-doughnut geometry in continuous OBRs and found that this geometry shows the highest values of shear strain rates, pressure drop and energy dissipation when compared with other geometries, such as the single orifice plate and diverse helical ribbon designs. However, interestingly, this design does not perform significantly better than the single orifice baffle in terms of radial mixing or axial dispersion. Sarkar et al. (2020) studied different variations of the disc-and-doughnut geometry: regular, slanted, concave, convex and inflexed. Based in their results, the convex disc-and-doughnut geometry provides low axial mixing; it is hence recommended for applications that do not require high shear rate or turbulence energy dissipation but require low axial dispersion. The inflexed geometry, on the other

hand, appears more suitable for the intensification of high shear applications, such as liquid-liquid extraction with systems having high interfacial tension and gas-liquid reactions or mass transfer operations.

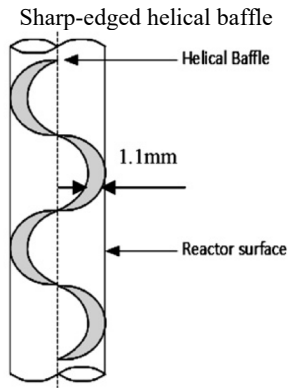
A number of variations of helical baffles have been proposed in the literature, including simple coiled wires, as well as single, double and alternating helical blades/ribbons to create sharp-edged helical baffles. Studies have shown that this geometry enables plug flow behaviour to be achieved over a wider range of oscillatory conditions than other geometries (McDonough et al., 2017; Phan and Harvey, 2011a, 2010). This has been explained by the additional swirl motion that is created from the interactions of the oscillatory flow and the helical baffle (Phan and Harvey, 2011a, 2010), which have been identified by different authors using numerical simulation (Mazubert et al., 2016a, 2016b; Solano et al., 2012) and PIV experiments (McDonough et al., 2017). However, the different helical baffles can provide differences in performance for varying applications due to their specific characteristics. For example, the sharp-edged helical baffle has been shown to provide better yield in the production of biodiesel than the coiled wire helical baffle due to the sharp edge, which generates higher shear rates and enables more effective liquid-liquid phase mixing (Phan et al., 2011b). Indeed, the helical baffle and alternating helical baffle provide improved plug flow behaviour compared with that generated by the single orifice and the disc-and-doughnut baffles, whilst maintaining significant levels of shear strain rate, which is important for droplet breakup (Mazubert et al., 2016a, 2016b). However, the vortical flow is less apparent in the alternating helical blade and the streamlines originating from the inlet appear to occupy less volume in the reactor (Mazubert et al., 2016a), suggesting that flow turnover close to the walls may be less efficient and potentially could hinder heat transfer at the wall.

Central baffles are periodically spaced discs mounted on an axial rod. This geometry offers higher shear rates and pressure drop compared with the single orifice baffle and smooth constriction geometries (Ahmed et al., 2018a), making it useful for homogeneous liquid-liquid reactions (Rasdi et al., 2013; Yussof et al., 2018). The wire wool and sharp-edge helical blade with central rod geometries have also demonstrated enhanced dispersion in liquid-liquid operations (Phan et al., 2012, 2011b). The helical coil baffle with central rod, also studied by McDonough et al. (2019a), has been shown to create a dual counter-rotating vortex regime due to the additional swirl velocity generated by the helical coils.

Table 1: Different baffled geometries used in OBRs.

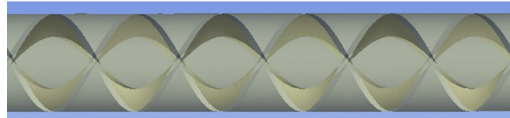
Baffled design	Reference
<p data-bbox="508 260 769 287">Single orifice (plate)</p> 	<p>(Mazubert et al., 2015; Ni et al., 2003a, 1998a; Stonestreet and Van Der Veecken, 1999)</p>
<p data-bbox="464 590 816 617">Single orifice (smooth constrictions)</p> 	<p>(Ahmed et al., 2018b; Eze et al., 2013; Phan and Harvey, 2010; Reis et al., 2005)</p>
<p data-bbox="521 810 756 837">Multi-orifice plate baffle</p> 	<p>(Ahmed et al., 2018b; González-Juárez et al., 2017; Lucas et al., 2016; Palma and Giudici, 2003; Smith and Mackley, 2006)</p>
<p data-bbox="480 978 797 1005">Tri-orifice baffle with central rod</p> 	<p>(Muñoz-Cámara et al., 2020; Nogueira et al., 2013; Soufi et al., 2017)</p>
<p data-bbox="516 1220 764 1247">Disc-and-doughnut baffle</p> 	<p>(Amokrane et al., 2014; Lobry et al., 2013; Mazubert et al., 2016a, 2016b; Sarkar et al., 2020)</p>
<p data-bbox="573 1566 704 1593">Helical baffle</p> 	<p>(Ahmed et al., 2018b; McDonough et al., 2019b, 2017; Phan and Harvey, 2011a, 2010)</p>





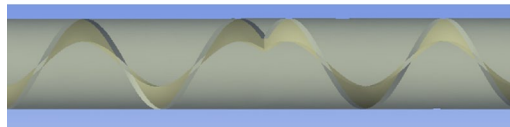
(Mazubert et al., 2016a, 2016b;  
Phan et al., 2011b; Phan and  
Harvey, 2011b)

Double helical baffle



(Mazubert et al., 2016a, 2016b)

Alternating helical ribbon



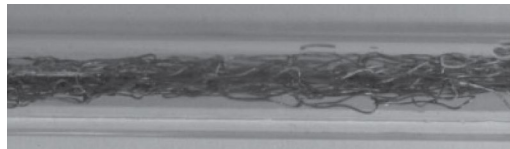
(Mazubert et al., 2016a, 2016b)

Central baffle



(Ahmed et al., 2018a;  
McDonough et al., 2019b; Phan et  
al., 2011a; Phan and Harvey,  
2010)

Wire wool



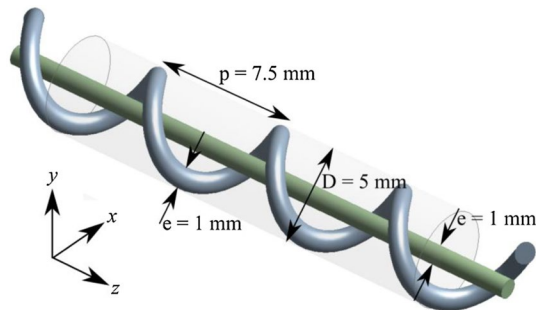
(Phan et al., 2012)

Sharp-edged helical with central rod



(Abdul et al., 2020; Phan et al.,  
2012, 2011b)

Helical baffle with central rod



(Horie et al., 2018; McDonough  
et al., 2019a)

### 2.1.2 Geometrical parameters

The geometrical parameters of the OBR influence the shape and size of the generated vortices, which require adequate space to fully expand and spread in each baffle cavity. The main geometrical parameters in the design of oscillatory baffled reactors are based on the single orifice baffle design; these are illustrated in Table 1 and summarized in Table 2. Table 2 gives the ranges of the most commonly used values, which were defined by the cited studies and are now often used as established design guidelines. However, it must be pointed out that these ranges of values were defined for specific conditions used in the original studies and have never been optimised for a wide range of operating conditions or applications.

Table 2: Summary of main geometrical parameters in oscillatory baffled reactor design.

Parameter	Symbol	Most commonly used values in the literature	References
OBR diameter	$D$	15 – 150 mm	----
Baffle spacing	$l_b$	$1.5D$	(Brunold et al., 1989)
Baffle orifice diameter	$d$	$0.45 – 0.5D$	(Ni et al., 1998a)
Dimensionless free baffle area	$\alpha$	$0.20 – 0.25$	(Ni et al., 1998a)
Baffle thickness	$\delta$	2 – 3 mm	(Ni et al., 1998a)
Oscillation amplitude	$x_o$	$0.25 – 0.6l_b$	(Gough et al., 1997; Soufi et al., 2017)

#### ***Tube diameter***

The selection of the diameter of the OBR depends on the process application and the desired production rate. In the literature, the conventional OBR diameter is typically in the range 15 mm to 150 mm. However, it should be pointed out that continuous flow OBRs offer the advantage of being able to ensure industrial-scale production rates even with 15 mm diameter reactors (Mazubert et al., 2015, 2014). In recent years, the interest in miniaturized OBRs (referred to as meso-OBRs in the literature) has increased. These miniaturized reactors have diameters of  $\leq 5$  mm and they are typically operated with lower flow rates than the larger-scale OBRs, allowing reduced material inventory and wastes. The smaller scale of meso-OBRs are particularly beneficial for rapid process screening and process development as explained by McDonough et al. (2015). Recent works show the feasibility of the use of meso-OBRs for multiphase reactions, such as solid-liquid carboxylic acid esterification (Eze

et al., 2017), hexanoic acid esterification (Eze et al., 2013), as well as gas-liquid ozonation of water and wastewater (Lucas et al., 2016).

### ***Baffle spacing, $l_b$***

The baffle spacing,  $l_b$ , is a key design parameter since it influences the shape and length of eddies within each baffle cavity (Brunold et al., 1989; Knott and Mackley, 1980). An adequate value of  $l_b$  ensures the full extension of the vortex generated behind the baffles, thus assuring its presence over the entire cavity between baffles. If the spacing between baffles is too small, the vortices hit adjacent baffles before their full expansion, resulting in a constrained growth of eddies, a reduction of radial motion, as well as undesirable axial dispersion in continuous operations (Brunold et al., 1989; Palma and Giudici, 2003). On the other hand, if the space between baffles is too large, the vortices do not occupy the full volume of the inter-baffle region. A spacing of  $l_b = 1.5D$  has been the most commonly used value in the literature following the single-phase flow visualization results reported by Brunold et al. (1989). Similar values have subsequently been recommended by others: Ni and Gao (1996b) reported an optimal value of  $l_b = 1.8D$  for their mass transfer studies, and Ni et al. (1998a) recommended a value of  $l_b = 2D$  in order to minimize mixing time in a batch OBR with oscillating baffles. It should be mentioned that the effectiveness of eddy generation and mixing is also inherently related to oscillation amplitude so the relationship between baffle spacing and oscillation amplitude is equally an important parameter.

For fixed values of inter-baffle spacing and orifice diameter,  $l_b$  and  $d$ , the combination of amplitude and frequency controls the generation and the propagation of eddies, producing different fluid flow behaviour. Gough et al. (1997) studied the effect of the oscillation frequency and amplitude on flow patterns by qualitative flow visualization in polymerisation suspensions in a OBR. It is important to point out that in this study, fluid oscillation was achieved by oscillating the baffles and not the fluid. From this study, the oscillation amplitude required to achieve similar flow patterns to those present in a conventional OBR (where the flow is pulsed) is approximately equal to  $0.25l_b$ . Even though, the operation of the reactor used in the study by Gough et al. (1997) is rather different from that of both batch and continuous flow OBRs, this relationship between baffle spacing and oscillation amplitude has been widely used for OBR design since that time. However, Reis et al. (2005) investigated a range of ratios of oscillation amplitude to baffle spacing (ranging from 0.015 to 0.85) and it was shown that flow separation could be achieved with amplitudes even lower than  $0.25l_b$ . More recently in an optimisation study carried out by Soufi et al. (2017), an amplitude of  $0.6l_b$ , which is significantly greater than the general design guideline, was found to give an optimal yield for a mass transfer limited

liquid-liquid reaction. Indeed, these authors put forth that the ‘optimal’ design of OBRs most certainly depends on the type of application (single phase, gas-liquid, solid-liquid etc.), the process objective and the performance parameter that is being optimized.

### ***Dimensionless free baffle area, $\alpha$***

The dimensionless free baffle area, defined as  $\alpha = \left(d/D\right)^2$ , impacts the size of eddies generated in each inter-baffle cavity. Small values of  $d$  will constrict the fluid more as it flows through the baffles, resulting in larger vortices, an increase in the pressure drop and improved mixing conditions. The dimensionless free baffle area is typically chosen in the range of 0.2–0.4 (Phan and Harvey, 2011b), but many studies have established a standardized orifice diameter of  $d = 0.5D$  (Abbott et al., 2014a; Mackley and Stonestreet, 1995; Navarro-Fuentes et al., 2019a; Ni et al., 1998a; Stonestreet and Harvey, 2002), which corresponds to a dimensionless free baffle area of  $\alpha = 0.25$ . Depending on if the flow is single or multiphase, different values of  $\alpha$  may be preferred. Ni et al. (1998a) studied the effect of dimensionless free baffle area for single phase flow on the mixing time in OBRs using either oscillating baffles or pulsed flow, over a range of  $0.11 < \alpha < 0.51$ . In both configurations (oscillating baffles and pulsed flow), the shortest mixing times were achieved for values of  $\alpha = 0.20 - 0.22$ . In liquid-solid flows, Ejim et al. (2017) stated that the dimensionless free baffle area plays a dominant role in controlling solid back-mixing and batch suspension of particles in meso-OBRs. In their study, a value of  $\alpha = 0.12$  was found to minimize axial dispersion, resulting in a longer mean residence time of the solids.

### ***Baffle thickness and size***

Other geometrical parameters, such as the baffle thickness and the gap between the baffle and the wall, also impact mixing performance. Ni et al. (1998a) demonstrated the influence of baffle thickness on the mixing efficiency and showed that vortex generation is favoured by thinner baffles. The authors observed an increase in mixing time as the baffle gets thicker, explained by the fact that if the time required for the vortices to cling to the baffle edge is too long prior to shedding (due to the increase in the baffle thickness), the vortex shape may only be slightly distorted, subsequently affecting the mixing time. Nevertheless, vortex deformation due to the baffle thickness has not been corroborated visually. However, thin baffles have less mechanical stability and it is expected that there would be a minimum

baffle thickness to diameter ratio ( $\delta/D$ ) that ensures the stability of baffles and vortex generation. The influence of the gap between the outer edge of the baffles and the tube wall on flow patterns was studied using particle image velocimetry (PIV) (Ni et al., 2004a). An increased gap results in the generation of smaller eddies and an increase in the axial velocity component compared with the radial component, thereby decreasing the mixing performance. It is interesting to note that this study does not specify if the area of the tube cross-section open to flow was kept constant as the gap increased (i.e., by reducing the orifice diameter) or not. Indeed, this is expected to be an important parameter, as for equal cross-sectional area open to the flow, it may be expected that higher axial dispersion would be obtained in geometries with no (or little) gap at the wall. Further work on this aspect is still to be addressed.

### 2.1.3 Further considerations

After close scrutiny of the current literature, the geometrical parameters and design guidelines, which are widely used and recommended for the operation of OBRs, have been – for the most part – based on ‘one-off’ studies using the single orifice baffle OBR and focussing on a particular application and performance parameter or qualitative observations. It is clear that for some designs, e.g., helical baffles and wire meshes, these established guidelines may not be applicable or may require modifications. Indeed, considering the variations in baffle geometries, additional design parameters may need to be considered, such as the disc diameter and the distance between the disc and the orifice for the disc-and-doughnut baffles, the effective tube diameter for the multi-orifice plate baffle, and the pitch, i.e., the axial distance of one complete helix turn (instead of the baffle spacing), for helical baffles.

## 2.2 Characteristic dimensionless groups

The key dimensionless groups that characterize the fluid mechanics and flow conditions in OBRs and pulsed flows are the net flow Reynolds number ( $Re_{net}$ ), oscillatory Reynolds number ( $Re_o$ ), Strouhal number ( $St$ ), the velocity ratio ( $\psi$ ) and the Womersley number ( $Wo$ ). These are presented in Table 3 and described briefly below.

### 2.2.1 Reynolds numbers

The net flow Reynolds number controls the flow pattern of the fluids (from laminar to turbulent flow), and is defined as the ratio of inertial forces to viscous forces:

$$Re_{net} = \frac{\rho u_{net} D}{\mu} \quad (1)$$

The oscillatory Reynolds number describes the intensity of mixing in the reactor. In  $Re_o$ , the characteristic velocity is the maximum oscillatory velocity:

$$Re_o = \frac{2\pi f x_o \rho D}{\mu} \quad (2)$$

Stonestreet and Van Der Veecken (1999) identified three different flow regimes: for  $Re_o < 250$  the flow is essentially two-dimensional and axi-symmetric with low mixing intensity; for  $Re_o > 250$  the flow becomes three-dimensional and mixing is more intense; finally, when  $Re_o > 2000$ , the flow is fully turbulent.

### 2.2.2 Strouhal number

The Strouhal number,  $St$ , describes oscillating flow behaviour and represents the ratio of the advection time to the characteristic time of the oscillations. If  $St \ll 1$ , the flow is more or less stationary. Traditionally, the Strouhal number is defined as  $St = fL/u$ , where  $f$  and  $L$  are the characteristic oscillation frequency and length scale, and  $u$  is the flow velocity. However Brunold et al. (1989) adapted the equation to oscillatory flow in a baffled tube as:

$$St = \frac{D}{4\pi x_o} \quad (3)$$

In this definition, the Strouhal number compares the effective eddy propagation distance via the oscillation amplitude with the tube diameter. However, this adapted definition of  $St$  eliminates oscillation frequency from the equation because the fluid velocity term is replaced with the maximum oscillatory velocity ( $2\pi f x_o$ ). However, the steadiness of the flow and eddy propagation also depend on the oscillation frequency and not exclusively on the oscillation amplitude. For this reason, the physical explanation of how higher values of  $St$  promote the propagation of the eddies to the next baffle (which is widely stated in the literature) remains unclear (Ahmed et al., 2017; McGlone et al., 2015; Phan and Harvey, 2011a).

The most common range of Strouhal numbers used in OBRs, as defined by equation (3), is  $0.15 < St < 4$  (Abbott et al., 2013). However, this common range may not necessarily be the best operating range for all processes. For example, Mazubert et al. (2014) observed a decrease in the conversion of waste cooking oil into methyl esters for  $St > 0.1$  and this was explained by poor liquid-liquid dispersion, due to the decrease of the probability for the reactive mixture to interact with baffles due

to low oscillation amplitude. It should be pointed out that surprisingly the baffle spacing,  $l_b$ , which influences the shape and length of eddies within each baffle cavity, is absent in the definition of  $St$  given in Equation (3), despite being strongly related.

### 2.2.3 Velocity ratio

The velocity ratio,  $\psi$ , describes the relationship between the oscillatory and net flow. It is typically recommended to operate at a velocity ratio greater than one to ensure that the oscillatory flow dominates the superimposed net flow (Stonestreet and Van Der Veecken, 1999). However, the recommended range of  $\psi$  to ensure plug flow operation (such that radial flow dominates and limits axial dispersion) is typically between two and four (Stonestreet and Van Der Veecken, 1999).

$$\psi = \frac{Re_o}{Re_{net}} \quad (4)$$

Nonetheless, this recommended velocity ratio range is not always used in practice; it is often adjusted with respect to the application and process objective, as well as the baffle design. Examples of this are discussed in Sections 3.1.1, 3.1.2, 3.1.3, 3.1.7.3, and 3.2.

### 2.2.4 Womersley number

The Womersley number ( $Wo$ ), which was originally proposed by John R. Womersley for blood flow in arteries, is widely used in characterisation of pulsatile flows (Womersley, 1955).  $Wo$  expresses the ratio of the oscillatory inertial forces to shear forces:

$$Wo = L \left( \frac{\rho\omega}{\mu} \right)^{\frac{1}{2}} \quad (5)$$

Interestingly,  $Wo$  is not frequently used in the characterisation of flow in OBRs, despite its utility in assessing the development of the pulsed flow. Typically, when the Womersley number is small ( $Wo < 1$ ), the frequency of oscillations is low enough to allow sufficient time for a fully developed flow profile to develop at each cycle. At high Womersley numbers ( $>10$ ), the frequency of the oscillating flow is too high to allow full flow development over a cycle and instead, the velocity profile is relatively flat or plug-like (Loudon and Tordesillas, 1998). Indeed, Slavnić et al. (2017) obtained narrower RTD and lower axial dispersion for higher frequencies, for the same amplitude ( $f = 1.75$  Hz and  $Wo = 43$ ). Hence, ensuring Womersley numbers higher than 10 could help for the proper selection of oscillatory conditions.

Table 3: Summary of main dimensionless groups in oscillatory baffled reactor design.

Parameter	Symbol	Recommended operating ranges	References
Net flow Reynolds number	$Re_{net}$	<ul style="list-style-type: none"> <li>• To achieve convection: <math>Re_{net} &gt; 50</math></li> <li>• No advantage of oscillation flow: <math>Re_{net} &gt; 250</math></li> </ul>	(Stonestreet and Harvey, 2002; Stonestreet and Van Der Veeken, 1999)
Oscillatory Reynolds number	$Re_o$	<ul style="list-style-type: none"> <li>• Flow 2D, axi-symmetric: <math>Re_o &lt; 250</math></li> <li>• Flow 3D, non axi-symmetric: <math>Re_o &gt; 250</math></li> <li>• Fully turbulent: <math>Re_o &gt; 2000</math></li> </ul>	(Stonestreet and Van Der Veeken, 1999)
Strouhal number	$St$	$0.15 < St < 0.4$	(Abbott et al., 2013)
Velocity ratio	$\psi$	<ul style="list-style-type: none"> <li>• Oscillatory flow dominates the superimposed net flow: <math>\psi &gt; 1</math></li> <li>• To ensure plug flow: <math>2 &lt; \psi &lt; 4</math></li> </ul>	(Stonestreet and Van Der Veeken, 1999)

### 3 Performance characterization

#### 3.1 Flow performance

Flow performance in OBRs can be characterised using many different measures, including flow patterns, velocity profiles, axial to radial velocity ratio ( $R_V$ ), plug flow behaviour (via the residence time distribution (RTD), the axial dispersion coefficient ( $D_{ax}$ ), or the Péclet number), mixing time, radial and axial fluid stretching, shear strain rate history, as well as swirl and radial numbers.

Whilst it has been shown in the literature that RTD measurements are an appropriate means to characterize mixing in OBRs for operations that require long residence times (e.g. crystallisation and polymerisation), other performance characteristics may need be taken into consideration when operating conditions are chosen for OBRs for other operations. Indeed, depending on the process objective, other characteristics may be important for quantifying mixing, such as the spatial homogeneity of a minor species or a second phase (e.g. solid suspension), shear strain rate for shear-sensitive applications (e.g. liquid-liquid dispersions, biological cultures) or even micromixing and how fast the fluids are mixed (Kukukova et al., 2009).

##### 3.1.1 Residence time distribution (RTD) and axial dispersion ( $D_{ax}$ )

One of the major flow performance indicators in continuous flow reactors is the residence time distribution. Indeed, characterisation of the plug flow behaviour via RTD and identification of the operating conditions that enable the narrowest RTD is important for chemical and physical processes.



RTD studies in OBRs are abundant in the literature (e.g. Abbott et al., 2014a; Dickens et al., 1989; Kacker et al., 2017; Mackley and Ni, 1991; Reis et al., 2004) and have most often analysed the impact of reactor geometry and flow conditions on the dispersion of a pulse injection of homogeneous tracer in a single phase. From these studies, it is apparent that various recommended ranges of  $\psi$  have been proposed to achieve plug flow depending on the size and the design of the OBR. For example: Stonestreet and Van Der Veecken (1999) proposed a range  $2 < \psi < 4$  using a 24 mm single orifice baffle OBR; Phan and Harvey (2010) found good plug flow in the ranges of  $4 < \psi < 8$  and  $5 < \psi < 10$  for a 5 mm meso-scale OBRs with either smooth constrictions or central baffles, respectively; Phan and Harvey (2011b) then found that plug flow could be achieved in a wider range of conditions ( $5 < \psi < 250$ ) when a helical baffle was used in the 5 mm meso-scale OBR.

The axial dispersion coefficient,  $D_{ax}$ , is a measure of the degree of deviation of flows from ideal plug flow, in which case  $D_{ax}$  should be equal to zero (Levenspiel, 2012). The one-dimensional axial dispersion convection-diffusion model is given by:

$$\frac{\partial C}{\partial t} = D_{ax} \frac{\partial^2 C}{\partial x^2} - u \frac{\partial C}{\partial x} \quad (6)$$

The dimensionless Péclet number can be used to express the axial diffusion coefficient. It represents the ratio of the convective to diffusive transport and is the reciprocal of the dimensionless axial dispersion coefficient defined as:

$$Pe = \frac{\bar{u}L}{D_{ax}} \quad (7)$$

Similar to the recommendations for other non-ideal continuous flow reactors, it is recommended that OBRs be operated such that a minimum value of  $D_{ax}/\bar{u}L$  is achieved in order to avoid significant deviation from plug flow. Reactors with  $Pe > 100$  present an ideal plug flow behaviour, while reactors with  $Pe < 1$  present an ideal perfectly mixed state (Hornung and Mackley, 2009).

Three different models – the tanks-in-series model without interaction (compartmental model), the tank-in-series model with backflow, and the dispersion model – have been used in the literature to interpret RTD data and predict the non-ideal behaviour of the OBR. Similar results can be obtained with any of the three models, although the tanks-in-series model is the most widely used in the literature due to its simplicity and robustness. However, the tanks-in-series model has to be used with caution since it is unable to represent back-mixing at higher values of  $x_o \cdot f$  ( $x_o = 0.23l_b$  and  $f = 20$  Hz) (Reis et al., 2010). This is explained by the fact that the backflow rates generated are not considered in the hydrodynamic model. In this case, the tank-in-series model with backflow or the dispersion model are recommended. It has been demonstrated many times that plug flow can be achieved in OBRs under

laminar flow conditions (i.e., low net Reynolds number) and the RTD can be controlled with the oscillatory conditions independently of the net flow, as can be observed in Figure 3 (Ni, 1995; Phan and Harvey, 2010; Reis et al., 2010; Stonestreet and Van Der Veecken, 1999). It can be seen in Figure 3 that the maximum number of tanks with the tanks-in-series model is reached at a velocity ratio between two and four for a single baffle orifice geometry at different net Reynolds numbers. Most of the recommended  $\psi$  values to achieve plug flow come from RTD data interpreted with the tank-in-series model, and the velocity ratios vary depending on the size and geometry of the OBR, as was discussed previously.

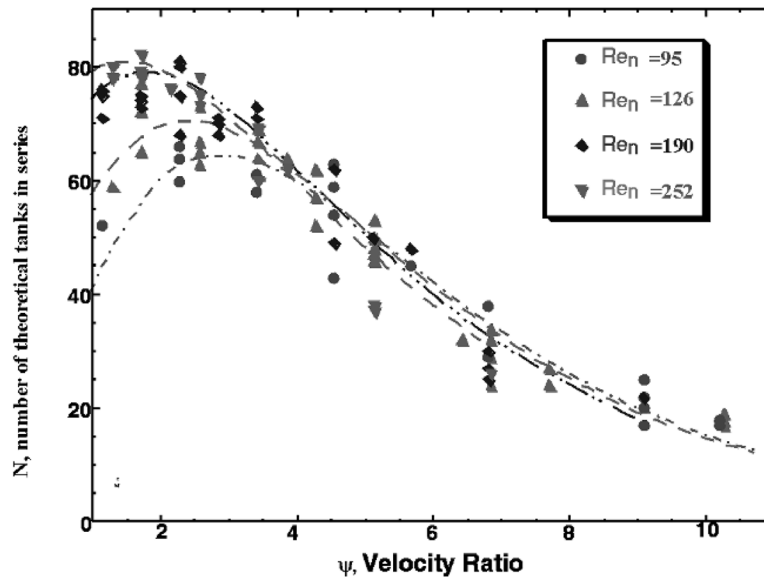


Figure 3 : The dependency of the tanks-in-series model parameter,  $N$ , on the oscillatory Reynolds number for different net Reynolds (Ni et al., 2003b).

Many studies have focused on the influence of the oscillatory frequency and amplitude on plug flow in OBRs. Palma and Giudici (2003) studied the influence of the pulsating frequency, amplitude and baffle spacing on the axial dispersion coefficient, by measurement of the RTD for single phase flow in OBRs with multi-orifice baffles. The results show that  $D_{ax}$  increases proportionally with an increase in the oscillatory velocity ( $x_o \cdot f$ ). However, it has further been shown that oscillation amplitude has a significant influence on RTD and axial mixing compared with the frequency, and that increasing oscillation amplitude increases  $D_{ax}$  (Dickens et al., 1989; Oliva et al., 2018; Slavnić et al., 2017). This is because the amplitude directly controls the length of the eddies generated along the tube (Hamzah et al., 2012). Smith and Mackley (2006) and González-Juárez et al. (2017) have also shown that multi-orifice baffles generally provide improved plug flow compared with single orifice baffles.

Indeed, an increase in the number of orifices leads to a decrease in  $D_{ax}$  (and hence an increase in the  $Pe$ ), thereby resulting in narrower RTD curves and improved plug flow behaviour.

### 3.1.2 Macromixing

Few studies have been addressed in OBRs concerning the macromixing quality of the reactor. For example, Ni et al. (1998a) characterized mixing in oscillatory baffled columns by determining the time necessary for a tracer to reach a specific uniform concentration in the column and provided design guidelines for free baffle area, baffle spacing and baffle thickness, as presented in Table 2. In recent studies, Avila et al. (2020a) studied the impact of the position of the tracer feed and flow conditions on the mixing quality of a continuous OBR. The spatial uniformity of the tracer was analysed using the areal distribution method developed by Alberini et al. (2014). It was found that for the single baffle orifice geometry, improved mixing was found when the tracer was introduced mid-way between the tube centreline and the wall. High velocity ratios  $> 4$  were recommended to obtain uniform spatial mixing rapidly, although this range is outside the usual recommended range of  $2 \leq \psi \leq 4$  to ensure plug flow. These results highlight the fact that different operating conditions may be required depending on the process objective.

### 3.1.3 Micromixing

Micromixing, i.e., mixing at the molecular scale, is the limiting step in the progress of instantaneous and competitive reactions. Poor micromixing can lead to a loss of conversion and the formation of undesired by-products (Baldyga and Pohorecki, 1995). Micromixing applications, such fast precipitation and crystallization, in OBRs are a challenging area because this kind of reactor does typically not provide fast micromixing conditions, and thereby leads to local segregation and a decrease in selectivity and/or product quality.

In a recent study, McDonough et al. (2019b) characterized micromixing in different meso-OBR geometries with the Villermaux-Dushman test reaction. They showed that both central baffles and smooth constrictions only enabled fast micromixing times for large velocity ratios where  $\psi > 25$ . However, these values of  $\psi$  are outside the recommended range for achieving plug flow in these geometries ( $4 < \psi < 10$ ) (Phan and Harvey, 2010). On the other hand, they showed that helical baffles provide both fast micromixing and plug flow over a much wider range of velocity ratios ( $5 < \psi < 250$ ) (Phan and Harvey, 2011a).

Nevertheless, due to the limited number of studies in this area, the effectiveness of micromixing in OBRs is not entirely clear. The impact of different operating conditions of reactant injection (such as inlet position and flow rate ratios), as well as how this interacts with the oscillatory flow and influences the micromixing performance in OBRs still needs to be explored. Additionally, the development of theoretical micromixing models that are better adapted to the interaction between oscillatory, net and reactant injection flows is important for a further comprehension of the micromixing phenomena in this kind of reactor, and the future implementation of OBRs for micromixing-controlled processes.

### 3.1.4 Velocity ratios

The axial to radial velocity ratio,  $R_V$ , allows quantification of the amount of axial flow ( $u_z$ ) compared with the transverse (or radial) flow ( $u_r$ ) created by the eddies.  $R_V$  decreases as transverse flow increases. It is determined over a plane or a volume using the velocity components from experimental or numerical flow fields (Ni et al., 2003a):

$$R_{VA}(t) = \frac{\sum_{j=1}^J \sum_{i=1}^I |u_{z(i,j)}| / J \cdot I}{\sum_{j=1}^J \sum_{i=1}^I |u_{r(i,j)}| / J \cdot I} \quad (8)$$

$$R_{VV}(t) = \frac{\sum_i |u_{i,z}| V_i}{\sum_i |u_{i,r}| V_i} \quad (9)$$

$$\text{where } u_{i,r} = \sqrt{u_x^2 + u_y^2}$$

Equation (8) is weighted by area, where  $J$  and  $I$  are the total number grid data points in the axial and radial directions, and equation (9) is weighted by volume. A number of studies have used  $R_V$  to analyse the flow performance of OBRs with single orifice baffles (Jian and Ni, 2005; Manninen et al., 2013; Mortazavi and Pakzad, 2020; Ni et al., 2003a; Sutherland et al., 2021). They observed that with increasing  $Re_o$ , transverse velocities increased, thereby decreasing  $R_V$ . Fitch et al. (2005) showed that  $R_V$  was found to decrease from a value of eight at very low  $Re_o$  to two at  $Re_o = 500$ . From their visual experimental results, they defined an empirical criterion of  $R_V < 3.5$  to achieve effective mixing. Nevertheless, due to the limited number of studies using the  $R_V$  criterion as an indicator of mixing, it is unclear whether this value may vary, since Fitch et al. (2005) reported a minimum value of  $R_V$  of two and Manninen et al. (2013) reported a value of one for the same baffle geometry. This may also be true concerning different baffle geometries. Mazubert et al. (2016a) found that the disc-and-doughnut and helical blade baffle geometries provide more effective radial mixing at low oscillatory Reynolds numbers than the single orifice plate geometry. Indeed, due to the presence of the disc in the

disc-and-doughnut geometry, the axial flow at the centreline is blocked causing a large vortical zone in front of and behind the disc at all moments of the oscillation cycle, thereby enhancing the radial flow component. The hydrodynamics of the helical blade baffles are more complex and they offer more radial mixing due to the generation of a highly three-dimensional flow, especially when flow reversal occurs, which is very different to the organised flow generated with the single orifice baffle geometry.

McDonough et al. (2017, 2019a) characterized mixing in an OBR with helical baffles with and without a central rod, using the swirl and radial numbers to identify whether mixing is dominated by swirl or vortex flows. The swirl number describes the ratio of the axial flux of angular momentum to the axial flux of linear momentum:

$$S_n = \frac{\int_z^v v_z v_\theta r^2 dr}{R \int v_z^2 r dr} \quad (10)$$

where  $v_z$  and  $v_\theta$  are the axial and tangential velocity components,  $r$  is the radial position, and  $R$  is the hydraulic radius. The radial number compares the axial flux of radial momentum with the axial flux of axial momentum:

$$r_n = \frac{\int_z^v v_z v_r r dr}{\int v_z^2 r dr} \quad (11)$$

These numbers can be plotted against the oscillatory velocity to show how the swirling and vortex strengths change during the oscillation cycle. They enable the transition between vortex-dominated mixing (i.e., at the peak of the radial component) and swirl-dominated mixing (i.e., at the peak of the swirl component) to be identified as the oscillation intensity increases. McDonough et al. (2017) have shown that these transitions agree well with the observations made in their experiments. The swirl and radial number are particularly well adapted to characterizing flow in helical baffle geometries due to the helical-shaped vortex formed behind the baffle and the dominant radial and tangential flows.

### 3.1.5 Heat transfer

OBRs have proven to significantly enhance heat transfer in both batch and continuous operation when compared with simple tubular reactors (Mackley and Stonestreet, 1995; Stephens and Mackley, 2002). The Nusselt number, which is the ratio of convective to conductive heat transfer, is often used to compare the performance between operating conditions and reactor geometries:

$$Nu = \frac{h_{OBR} D}{k} \quad (12)$$

where  $h_{OBR}$  is the OBR-side transfer coefficient and  $k$  the thermal conductivity of the process fluid.

When an oscillatory flow is applied to the net flow, it has been shown that the Nusselt number is enhanced up to 30-fold, depending on the oscillatory conditions, net flow, fluid properties and OBR geometry (Ahmed et al., 2018a; González-Juárez et al., 2018; Law et al., 2018; Mackley and Stonestreet, 1995; Ni et al., 2003b; Onyemelukwe et al., 2018; Solano et al., 2012). As illustrated in Figure 4, the effect of oscillatory flow on heat transfer is significant in the laminar flow regime ( $Re_{net} < 1000$ ) and the highest values of  $Nu$  are obtained at high  $Re_o$ . However, the impact of  $Re_o$  on heat transfer decreases as  $Re_{net}$  increases. Indeed, the curves start to converge to the steady-state behaviour ( $Re_o = 0$ ) as  $Re_{net}$  starts to dominate and the benefits of the oscillatory flow are lost. The enhancement of the heat transfer rate is attributed to the chaotic flow structures created by the oscillatory flow interacting with the cold and hot flows, and by obtaining the maximum value of  $Nu$  during the formation of the vortex behind the baffle (Solano et al., 2012). The helical baffle design has shown to provide highest heat transfer performance when compared with other geometries (Ahmed et al., 2018a). The characteristic swirl-radial motion and vortex-travelling structures generated by the helical baffles, as described by McDonough et al. (2017), greatly contribute to flow renewal at the wall, thereby enhancing the heat transfer coefficient.

Heat transfer performance has shown to be more dependent on the Strouhal number (and therefore oscillation amplitude) than the oscillation frequency alone, and heat transfer performance decreases for  $St < 0.8$  in a 5 mm OBR with smooth constrictions (Onyemelukwe et al., 2018). This can be related to the axial dispersion in the reactor since, as was already discussed, an increase in oscillation amplitude increases  $D_{ax}$  and plug flow behaviour decreases. These results, however, contradict those reported by Mackley and Stonestreet (1995) and González-Juárez et al. (2018) for larger sharp-edged baffled reactors with tube diameters of 12 mm and 25 mm, respectively. They found the frequency has a strong effect on the heat transfer rather than the amplitude. This disagreement may be attributed to the difference in scale of OBRs. Indeed, the effect of the surface to volume ratio plays an important role when comparing heat transfer in different OBR sizes; however, this has not been specifically addressed in these works.

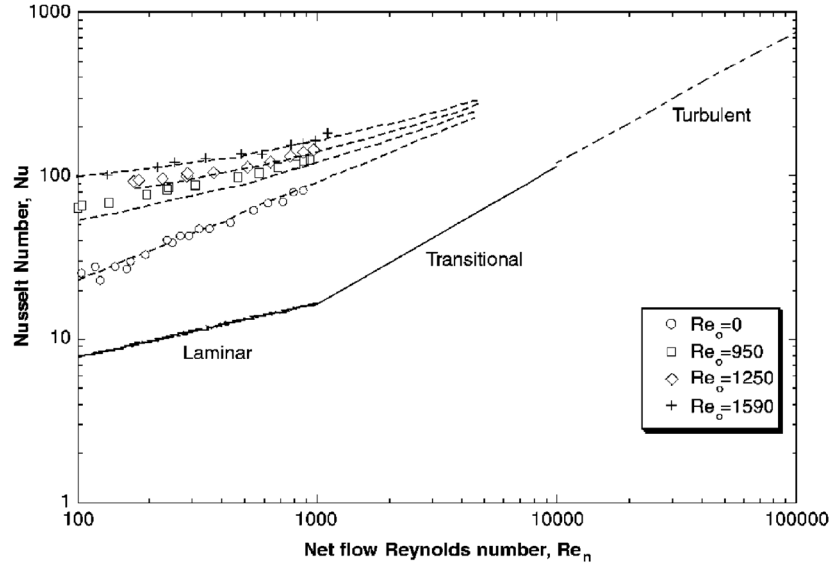


Figure 4: Heat transfer enhancement in oscillatory baffled tubes, adapted from the work of Mackley and Stonestreet (1995) (Ni et al., 2003b).

Different correlations have been proposed to predict the Nusselt number in OBRs over recent years. The first and most well-known phenomenological correlation was given by Mackley and Stonestreet (1995) for the range  $100 \leq Re_{net} \leq 1200$  and  $Re_o \leq 800$ :

$$Nu = 0.0035 Re_{net}^{1.3} Pr^{1/3} + 0.3 \left[ \frac{Re_o^{2.2}}{(Re_{net} + 800)^{1.25}} \right] \quad (13)$$

The first term corresponds to the steady-state flow contribution and was chosen to be like the Dittus-Boelter turbulent flow correlation, however the value of the exponent is higher in order to take into account the fluid recirculation due to the presence of the baffles. The second term corresponds to the oscillatory flow contribution, assuming that when  $Re_o \gg Re_{net}$  the influence of oscillations is superimposed on the steady behaviour and that the oscillatory term can be added to the steady-state term. In the case when  $Re_{net} \gg Re_o$ , the influence of the oscillations is small and the correlation reduces to that for steady-state behaviour. The influence of the Prandtl number on the Nusselt number was not determined in the study.

Until the end of the 2010s, no other significant correlation was proposed for the prediction of heat transfer in OBRs. However, several studies have been carried out to obtain more robust Nusselt number correlations in the last few years. Table 4 presents a summary of the correlations available in the current literature. Whilst the correlations are similar, the constants and exponents are strongly dependent on the geometry, operating conditions and working fluid. González-Juárez et al. (2018) compared their heat transfer data obtained in a OBR with single orifice baffles with the correlations proposed by

Mackley and Stonestreet (1995) and by the Polymer Fluid Group from Cambridge University for a range  $5 \leq Re_{net} \leq 1000$ . It was generally found that these correlations did not provide the same results and neither correlations correctly represent the experimental results obtained by González-Juárez et al. (2018) for  $Re_{net} < 500$ , however the agreement was slightly better at higher  $Re_{net}$  ( $> 500$ ).

Onyemelukwe et al. (2018) presented an additional correlation for heat transfer in a meso-OBR with smooth constrictions. This correlation follows the same principle of Mackley and Stonestreet's (1995) correlation with the difference that the coefficient of the first term is higher due to the significant influence of the net flow on the heat transfer rate, and the inclusion of  $St$  independently of  $Re_o$ .

Ahmed et al. (2018a) also proposed general heat transfer correlations for three meso-OBR designs, following the equations established by Law et al. (2018), which are analogous to the Dittus-Boelter correlation but have an additional term involving  $Re_o$ . The coefficient of the correlations depends on the tube diameter and baffle geometry, making the equations more versatile and robust for the prediction of Nusselt numbers. They also show good agreement with the correlations proposed by Mackley and Stonestreet (1995) and Law et al. (2018).



Table 4: Correlations for tube-side Nusselt number found the literature.

Geometry	Range of applicability	Correlation	Reference
Single orifice plate baffle $D = 12$ mm $\alpha = 0.35$ $l_b = 1.5D$	$100 \leq Re_{net} \leq 1200$ $Re_o \leq 800$ $Pr = 73$	$Nu = 0.0035 Re_{net}^{1.3} Pr^{1/3} + 0.3 \left[ \frac{Re_o^{2.2}}{(Re_{net} + 800)^{1.25}} \right]$	(Mackley and Stonestreet, 1995)
Single orifice plate baffle $D = 24$ mm $\alpha = 0.25$ $l_b = 1.5D$	$Re_{net} \leq 1000$ $Re_o \leq 1590$ $Pr = 73$	$Nu = Pr^{1/3} \left[ 0.36 Re_{net}^{0.6} + 0.8 \frac{Re_o^{1.7}}{Re_{net} + 10,000} \right]$	(Paste, Particle and Polymer Processing Group (P4G), accessed February 17, 2020)
Smooth constriction baffle $D = 5$ mm $\alpha = 0.16$ $l_b = 2.6D$	$11 \leq Re_{net} \leq 54$ $Re_o \leq 197$ $Pr = 5.37$	$Nu = 0.01616 Re_{net}^{1.16} Pr^{1/3} + 0.0016 \left[ Re_o^{0.08} Re_{net}^{1.42} \frac{St}{1.136} \right]$	(Onyemelukwe et al., 2018)
Single orifice plate baffle $D = 26.2$ mm $\alpha = 0.246$ $l_b = 2D$	$200 \leq Re_{net} \leq 1300$ $Re_o \leq 8700$ $4.4 \leq Pr \leq 73$	For $Re_o \leq 1300$ $Nu = 0.022 Re_{net}^{0.7} Pr^{1/3} Re_o^{0.44}$  For $Re_o > 1300$ $Nu = 0.52 Re_{net}^{0.7} Pr^{1/3}$	(Law et al., 2018)
OBRs $D = 5$ mm $l_b = 1.5D$ <u>Helical baffle</u> $\alpha = 0.59$ <u>Central baffle</u> $\alpha = 0.13$ <u>Single orifice plate baffle</u> $\alpha = 0.25$	$61 \leq Re_{net} \leq 2400$ $Re_o \leq 1550$ $Pr = 4.4$	For $Re_o \leq 1300$ $Nu = \lambda Re_{net}^{0.7} Pr^{1/3} Re_o^{0.44}$  For $Re_o > 1300$ $Nu = 23.45 \lambda Re_{net}^{0.7} Pr^{1/3}$  Meso-helical baffle: $\lambda = 0.009$ Meso-central baffle: $\lambda = 0.011$ Meso-single orifice baffle: $\lambda = 0.007$	(Ahmed et al., 2018a)
Tri-orifice baffle with central rod $D = 32$ mm $D_e = 15.5$ mm $\alpha = 0.25$ $l_b = 2.6D_e$	$10 \leq Re_{net} \leq 600$ $Re_o \leq 600$ $190 \leq Pr \leq 470$ $\psi > 1$	$Nu = 0.412 Re_{net}^{0.196} Re_o^{0.583} Pr^{0.285}$	(Muñoz-Cámara et al., 2020)

### 3.1.6 Energy dissipation rate

The energy dissipation rate is considered a key parameter in industrial processes, since it influences mass and heat transfer, mixing quality and scale-up guidelines. In practice, energy dissipation rate in continuous flow equipment is determined by pressure drop measurements, generally with pressure transducers installed in the pipe upstream and downstream of the OBR. This usually leads to additional fittings, valves and bends and making it hence difficult to calculate power density in the continuous OBR alone. Other related problems concerning the calculation of power consumption, like the pressure drop along the reactor and the influence of the superimposed oscillatory flow on the oscillator and pumps have been recently studied. Jimeno (2019) found using numerical simulation that the average value of the power density and maximum center-to-peak pressure drop ( $\Delta p/L$ ) over an oscillation period remain constant over the reactor length, which is to be expected due to the periodic geometry. They also observed local energy losses that vary during the oscillation period. Muñoz-Cámara et al. (2021) further proposed different interaction correction factors, which consider the nonlinear effect of the oscillatory flow on the net pump power and the net flow on the oscillator power consumption. These factors allow the correct selection and installation of the net flow pump and the oscillator engines.

Due to the potential technical difficulties related to the measurement of power consumption as mentioned above, past studies on energy dissipation rate have mainly been based on the use of analytical and empirical models (Baird and Stonestreet, 1995; Jealous and Johnson, 1955; Mackley and Stonestreet, 1995; Muñoz-Cámara et al., 2021), and more recently CFD simulations (Avila et al., 2020b; Jimeno, 2019; Jimeno et al., 2018; Sutherland et al., 2020). The analytical and empirical models are themselves based on a number of hypotheses, which will be detailed further below. On the other hand, the determination of energy dissipation rate via CFD is a direct method.

The power consumption in oscillatory flows can be characterised by the time-averaged power consumption over an oscillation period divided by the volume of the reactor. The quasi-steady flow model (QSM) by Jealous and Johnson (1955) and the eddy enhancement model (EEM) by Baird and Stonestreet (1995) are two models that are found in the literature for estimating the energy dissipation rate in oscillatory flows in pulsed batch columns and in oscillatory flow in tubes with no net flow, and both assume high oscillatory velocities and a turbulent flow regime. These models are the only ones that have been employed for estimating power dissipation in OBRs since the 1990s.

The quasi-steady flow model is based on the standard pressure drop relation across a simple sharp-edged orifice, and assumes that the instantaneous pressure drop in an oscillation period is the same as the pressure drop that would be achieved in steady-state flow with the same velocity:

$$\left(\frac{P}{V}\right)_{QSM} = \frac{2\rho n(\omega x_o)^3(1/\alpha^2 - 1)}{3\pi C_D^2 L} \quad (14)$$

The discharge coefficient ( $C_D$ ) depends on the regime of the flow. In turbulent flow and for simple orifices with sharp edges, the value of the coefficient varies between 0.6 and 0.7; while for laminar flow,  $C_D$  varies with the ratio of the reactor diameter to orifice diameter ( $D/d$ ), and it is proportional to  $\sqrt{Re}$ . (Johansen, 1930; Liu et al., 2001). This, in addition to the fact that the model was developed for low oscillation frequencies  $f$  (0.5–2 Hz) and high oscillation amplitudes  $x_o$  (5–30 mm), limits its application to the OBRs geometry with sharp orifice baffles and specific flow conditions. The model also assumes that there is no pressure recovery between orifice baffles, due to the short distance between them. This assumption has recently been examined by Jimeno et al. (2018) who found that some pressure recovery does indeed take place when the baffle spacing is equals to  $1.5D$  or greater.

The eddy enhancement model is based on the prediction of frictional pressure drop as the acoustic resistance of a single orifice plate (Baird and Stonestreet, 1995). The EEM replaces the kinematic viscosity with eddy kinematic viscosity for turbulent flow. This model was proposed for high frequencies  $f$  (3–14 Hz) values and low oscillation amplitudes  $x_o$  (1–5 mm), being the opposite to the QSM. It includes an adjustable empirical parameter corresponding to the turbulent scale, the mixing length ( $l$ ), which is expected to be of the same order as the OBR diameter:

$$\left(\frac{P}{V}\right)_{EEM} = \frac{1.5\rho\omega^3 x_o^2 l}{\alpha l_b} \quad (15)$$

In addition to the dependency of the mixing length on the reactor geometry, Reis et al. (2004) reported that  $l$  is also depends on oscillation amplitude. This indeed limits the use of this model for a wide range of conditions and reactor designs.

Both models have been used to compare performances between traditional stirred-tank reactors and OBR for different applications, such as bioprocesses and crystallization (Abbott et al., 2014b; Ni et al., 2004b). Despite the recommended oscillatory conditions of each model, the QSM model has been the most widely used of the two. Many studies have used the QSM rather than the EEM, and a number of them use it outside the original recommended range of frequency and amplitude (Ahmed et al., 2018b; Callahan and Ni, 2014; Ejim et al., 2017; Siddique et al., 2015; Slavnić et al., 2019; Yang et al., 2015). Unfortunately, there exists limited fundamental studies of energy dissipation rate in OBRs – probably due to the difficulties in measurement – therefore limiting the validation of both models. Few studies have been carried out on this subject (Avila et al., 2020b; Jimeno, 2019; Jimeno et al., 2018; Mackley and Stonestreet, 1995; Muñoz-Cámara et al., 2021; Sutherland et al., 2020). Mackley and Stonestreet

(1995) proposed the use of a correction factor in the QSM to consider the power density provided by the net flow:

$$\varphi = \left[ 1 + 4 \left( \frac{Re_o}{\pi Re_{net}} \right)^3 \right]^{1/3} \quad (16)$$

Nevertheless, the use of this factor is limited because its physical meaning remains unclear.

Jimeno et al. (2018) used the QSM and EEM models to calculate the power density in a smooth constriction baffle OBR. The results were compared with CFD simulations of turbulent flow through the pressure drop across the reactor, and they found that the QSM overestimate the energy dissipation rate due to inadequate values of geometrical parameters such as  $n^*$  and  $C_D$ , while the EEM provides better agreement. Both models were then modified by adjusting the geometrical parameters and proposing an empirical correlation for mixing length:

$$\left( \frac{P}{\bar{V}} \right)_{QSM*} = \frac{2\rho n^{0.7} (\omega x_o)^3 (1/\alpha^2 - 1)}{3\pi C_D^2 (V/A)} \quad (17)$$

$$\left( \frac{P}{\bar{V}} \right)_{EEM*} = \frac{1.5n^{0.7} \rho \omega^3 x_o^2 l^*}{\alpha (V/A)} \quad (18)$$

$$l^* = 0.002 \left[ \alpha^2 \frac{d}{\pi x_o} \right]^{0.57} \quad (19)$$

With these modifications, the new models predict similar energy dissipation rates in turbulent flow for a wide range of operating conditions, being in good agreement with the authors' CFD simulations. However, due to the presence of adjustable parameters based on reactor geometry in the modified models, it is expected that the values of these parameters would need to be changed if the reactor geometry and/or baffle design were modified.

Recently, Avila et al. (2020b) determined the power density in an OBR with smooth orifice baffles for a range of operating conditions in laminar flow. They proposed an alternate method to predict power consumption by plotting dimensionless power density  $(P/V)^*$  as a function of a Reynolds number based on the sum of both the oscillatory and net flow velocities,  $Re_T$ . This approach is analogous to friction factor plots for flow in pipes and power number plots for stirred tanks. As shown in Figure 5,  $(P/V)^*$  is inversely proportional to  $Re_T$  in laminar flow and constant in turbulent flow. The proportionality constant in equation (23) and the constant in equation (24) are geometry dependent (as is the case for the power number of an impeller in a stirred tank). However, once the master curve for a specific OBR geometry is generated,  $P/V$  can be calculated from the operating conditions alone. For

this approach to be of more extended use, further work in the determination of master plot for OBRs with other baffle geometries is required.

$$Re_T = \frac{(2\pi f x_o + u_{net})\rho D}{\mu} \sqrt{\frac{\beta}{\alpha}} \quad (20)$$

$$\beta = \frac{l_b^{opt}}{l_b} \quad (21)$$

$$\left(\frac{P}{V}\right)^* = \frac{(P/V)D}{\rho(2\pi f x_o + u_{net})^3} \quad (22)$$

$$(P/V)^* = 330/Re_T \quad \text{for laminar flow } (\alpha = 0.25 / l_b = 1.1D) \quad (23)$$

$$(P/V)^* = 1.92 \quad \text{for turbulent flow } (\alpha = 0.22 / l_b = 1.6D) \quad (24)$$

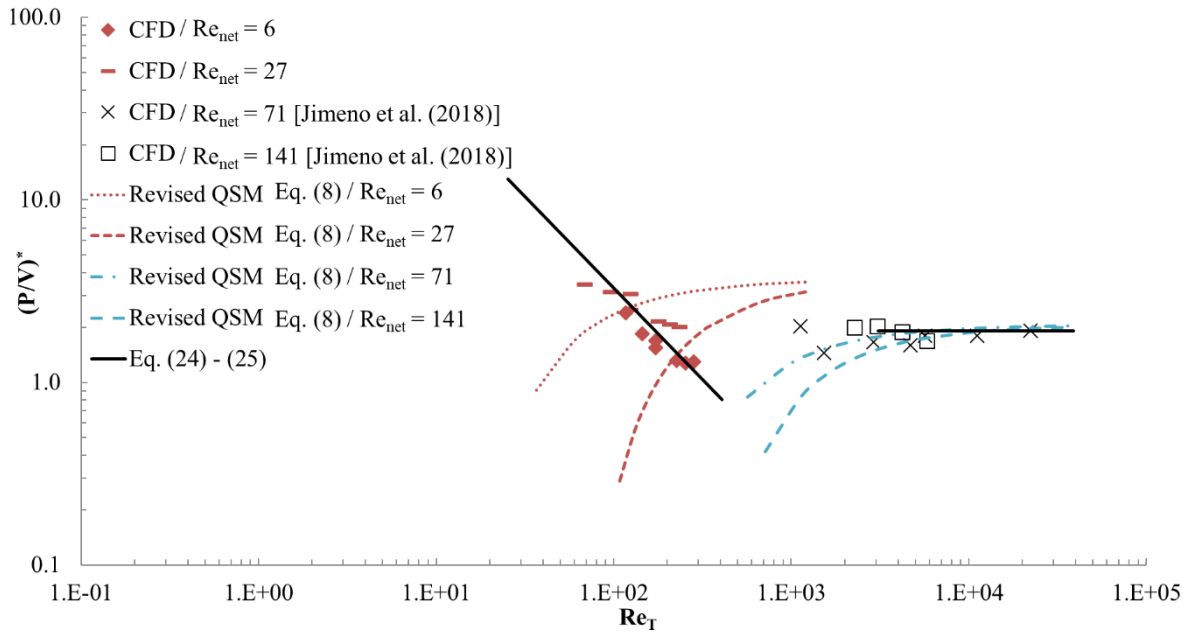


Figure 5: Dimensionless power density number as function of  $Re_T$  (Avila et al., 2020b).

### 3.1.7 Advances in multiphase systems

#### 3.1.7.1 Gas-Liquid systems

Many studies in the literature have compared the mass transfer performance of OBRs with conventional gas-liquid contactors, such as STRs and bubble columns. These have shown that a significantly higher number of smaller bubbles and therefore increased  $k_L a$  values are obtained in OBRs for various combinations of baffle spacing, amplitude and frequency (Ahmed et al., 2018b; Al-Abduly et al., 2014; Ferreira et al., 2015; Hewgill et al., 1993; Ni and Gao, 1996b; Oliveira and Ni, 2001; Pereira et al., 2014; Reis et al., 2007). For example, Hewgill et al. (1993) reported an increase in the mass transfer

coefficient by up to six-fold for an air-water system compared with conventional STRs (illustrated in Figure 6), whilst Al-Abduly et al. (2014) found that  $k_L a$  for ozone-water transfer in OBRs are more than five and three times greater than that observed in bubble and baffled columns, respectively.

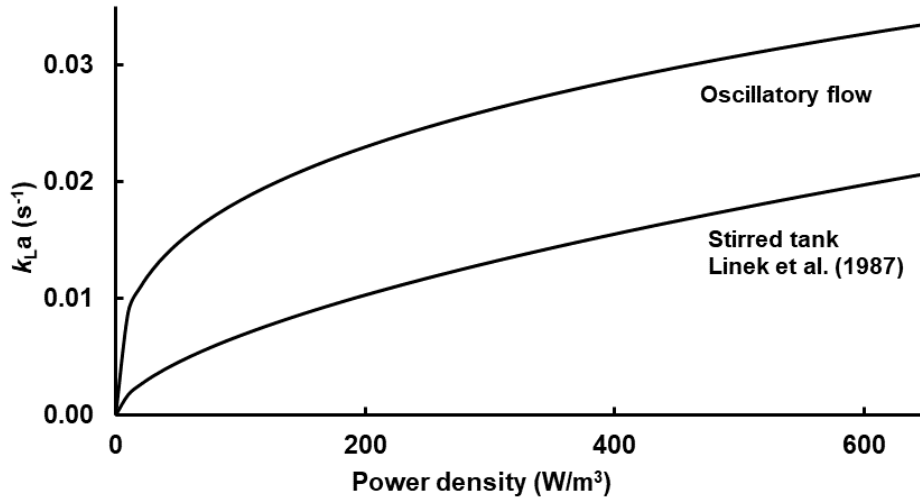


Figure 6:  $k_L a$  as a function of power density for a 50 mm diameter OBR with single orifice baffles and a STR at constant superficial gas velocity (Hewgill et al., 1993).

The reason for the increase in gas-liquid mass transfer in OBRs was studied by Oliveira and Ni (2001). They characterized gas-liquid flow patterns experimentally in a single orifice baffle OBR and studied the influence of oscillatory conditions on gas hold-up and bubble size. The bubbles were found to interact strongly with the eddies created by the presence of the baffles, and the high radial mixing and the detachment mechanism of vortex rings from the walls were found to be the reasons for the increased bubble retention and effective gas-liquid contacting area. As the oscillatory velocity increases, intermediate-scale vortices formed by the interaction of oscillatory flow and the baffles cause bubble breakup, thereby increasing the gas-liquid surface area. These vortices also retain bubbles for a longer time, thereby increasing the gas-phase residence time and gas hold-up. It was further shown that gas hold-up has greater impact on the volumetric transfer rate than bubble size (Oliveira and Ni, 2004). Whilst this observation may contradict the behaviour of gas-liquid mass transfer in conventional STRs, it is explained by the fact that the decrease in the bubble size causes the bubbles to become more rigid with less fluid circulation at the interface, thereby resulting in a reduction of the liquid-side mass transfer coefficient. This effect is outweighed by the observed increase in the interfacial area. As a direct consequence of these opposing effects, the bubble size plays a much less important role in the enhancement of mass transfer than the gas holdup.

Among the different OBR geometries, the multi-orifice baffles result in higher mass transfer coefficients compared with the single orifice baffle geometry. This is certainly due to the fact the gas phase is forced through much smaller orifices in the former geometry, thereby increasing shear strain rates and promoting bubble breakup, as well as enhanced recirculation and hold-up. On the other hand, the helical baffle design has not shown any significant improvement in the mass transfer coefficient, making it less useful for gas-liquid mass transfer applications (Ahmed et al., 2018b; Pereira et al., 2014).

### **3.1.7.2 Liquid-Liquid dispersions**

Liquid-liquid dispersion is a key operation in many processes, including both liquid-liquid reactions and extractions. Good control of the mean droplet size and droplet size distribution defines the quality and properties of the final product and the process performance. Inspired by pulsed extraction column processes (Angelov and Gourdon, 2012; Golding and Lee, 1981; Karr, 1959; Kumar and Hartland, 1988; van Delden et al., 2006), liquid-liquid dispersions have been widely studied in OBRs. It has been demonstrated that the oscillatory flow plays a more significant role in the control of the mean droplet diameter and size distribution than the net flow (Lobry et al., 2013). Furthermore, an increase in either the amplitude or the frequency decreases the droplet size and narrows the distribution (Lobry et al., 2014, 2013; Ni et al., 2001b, 1999, 1998b; Pereira and Ni, 2001), as it can be observed in Figure 7(a). Indeed, the oscillatory velocity was shown to control the breakage rate, with the amplitude having a more significant effect than the frequency (Mignard et al., 2006, 2004). On the other hand, the net flow has shown to not have a significant effect on the size and distribution of the droplets, as shown in Figure 7(b) (Lobry et al., 2013). This is of particular interest since it means that that residence time can be controlled and modified without modifying the properties of the liquid-liquid dispersion.

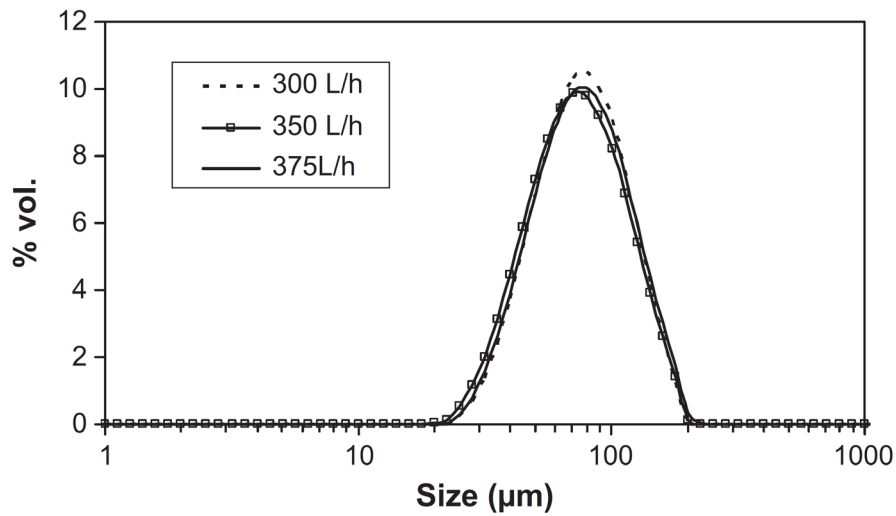
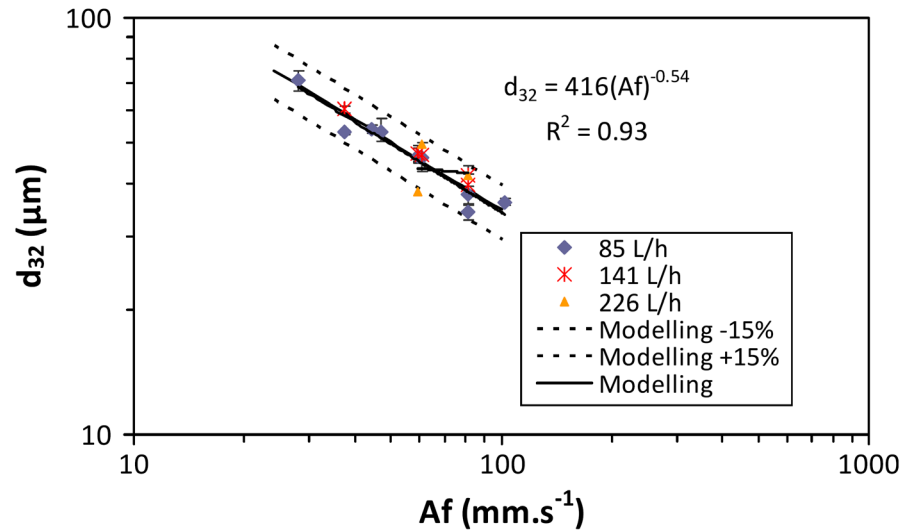


Figure 7: (a) mean droplet size as function of oscillatory velocity, with  $A = x_o$ , (b) droplet size distribution for different net flowrates and the same oscillatory conditions ( $x_o = 52$  mm and  $f = 1.17$  Hz) (Lobry et al., 2013).

Many correlations for mean droplet size can be found in the literature, as given in Table 5. The mean droplet size is usually presented as a power-law expression in terms of the oscillatory velocity ( $x_o \cdot f$ ) or oscillatory Reynolds number. Pereira and Ni (2001) proposed a correlation where the net Reynolds number is considered, however, since the oscillatory flow plays a more dominant role in the controlling the mean droplet diameter than the net flow, the coefficient on the net flow terms is lower than those of the oscillatory term. Indeed, as long as the oscillatory flow dominates over the net flow, the correlations proposed by (Ni et al., 2001b, 1998b) may be preferred.

Most of the correlations do not take the influence of fluid properties, such as interfacial tension, viscosity and density, into account. However, under identical oscillatory conditions and reactor



geometry, different droplet sizes have been found for different fluids (Lobry et al., 2013). Such differences may be attributed to different fluid properties (which can affect interfacial tension) and interaction with reactor material (i.e., surface wettability), and these will modify the droplet size. Lobry et al. (2014, 2013) integrated the impact of fluid properties into their correlations by including the Weber number, which represents the ratio between the inertial and interfacial forces. These are therefore recommended for a generalised prediction of the mean droplet size in OBRs.

Table 5: Mean droplet size correlations for oscillatory baffled reactors.

Geometry	Range of applicability	Correlation	Reference
Single orifice plate baffle $D = 50$ mm $\alpha = 0.19$ $l_b = 1.5D$	$1 \leq x_o \leq 15$ mm $1 \leq f \leq 10$ Hz $0.75 \leq P/V \leq 44$ W kg <sup>-1</sup>	$d_{32} = 0.996 \times 10^{-6} (x_o f)^{-1.2}$ (m) $d_{32} = 6.80 \times 10^{-5} (P/V)^{-0.4}$ (m)	(Ni et al., 1998b)
Single orifice plate baffle (pulsed baffles) $D = 50$ mm $\alpha = 0.23$ $l_b = 1.5D$	$10 \leq x_o \leq 50$ mm $1 \leq f \leq 5$ Hz $10 \leq P/V \leq 90$ W kg <sup>-1</sup>	$d_{32} = 2.8 \times 10^{-5} (x_o f)^{-0.96}$ (m) $d_{32} = 7.26 \times 10^{-4} (P/V)^{-0.32}$ (m)	(Ni et al., 2001b)
Continuous single orifice plate baffle $D = 40$ mm $\alpha = 0.21$ $l_b = 1.8D$	$0 \leq x_o \leq 60$ mm $0 \leq f \leq 5$ Hz $250 \leq Re_{net} \leq 1000$ $3.18 \leq P/V \leq 25$ W kg <sup>-1</sup>	$d_{32} = 1.72 \times 10^{-2} Re_o^{-0.91} Re_{net}^{-0.42}$ (m) $d_{32} = 3.7 \times 10^{-5} (P/V)^{-0.3} (P/V)_n^{-0.14}$ (m)	(Pereira and Ni, 2001)
Continuous disc and doughnut baffle $D = 50$ mm $\alpha = 0.25$ $l_b = 0.48D$	$24 \leq x_o \leq 52$ mm $1.17 \leq f \leq 1.56$ Hz $2600 \leq Re_o \leq 10\ 200$ $2190 \leq Re_{net} \leq 2675$	$\frac{d_{32}}{D} = 5 Re_o^{-0.85} We_s^{-0.26}$	(Lobry et al., 2013)
Continuous smooth reduction baffle $D = 15$ mm $\alpha = 0.28$ $l_b = 1.7D$	$10 \leq x_o \leq 70$ mm $0.35 \leq f \leq 1.4$ Hz $800 \leq Re_o \leq 3200$ $180 \leq Re_{net} \leq 300$	$\frac{d_{32}}{D_h} = 2.99 Re_{oh}^{-0.89} We_h^{-0.08}$	(Lobry et al., 2014)

### 3.1.7.3 Liquid-Solid suspensions

Liquid–solid flows are important in crystallization and catalytic reactions, where the size and distribution of particles, as well as the suspension of the solids and kinetic rates are directly affected by the mixing behaviour of the solids and fluid.

Solid-liquid flow patterns were analysed by Slavnić et al. (2019), who identified four flow regimes: creeping solid flow, dense solid flow, dilute solid flow and solid washout. In the creeping solid flow, particles were moving very slowly and were not effectively suspended. In dense solid flow, a considerable number of particles are transported in between the baffles, but they are still not uniformly dispersed in the tube. For the dilute solid flow regime, higher amounts of solids move from one inter-baffle compartment to the next in a near-uniform suspension. Finally, in the solid washout flow regime,

the oscillatory axial velocity dominates over the particle settling velocity and the solids are washed out of the reactor. An increase in the amplitude and/or frequency leads to a change in the flow regime, as well as to a decrease in the axial dispersion of solids, the ratio of solids to liquid mean residence time and the solids hold-up.

The presence of oscillatory flow has been shown to have positive impacts on solid-liquid flows. Oscillatory flow enables the suspension of sedimenting particles (Mackley et al., 1993) and with an increase in amplitude and/or frequency, a more uniform particle suspension is achieved (Ejim et al., 2017). Additionally, particle mixing has been found to be very sensitive to the frequency and amplitude of oscillations, hence allowing good control of the required mixing state by fine-tuning these operating conditions (Kacker et al., 2017; Reis et al., 2005). In particular, particles are easier to suspend at higher frequencies and lower amplitudes, which is also advantageous for obtaining plug flow behaviour in solid-liquid suspensions (Kacker et al., 2017; Reis et al., 2005). It is interesting to point out that whilst the recommended range of velocity ratio,  $\psi$ , to ensure plug flow in single phase liquid systems has been reported to be between two and four (Stonestreet and Van Der Veecken, 1999), higher values are typically required for solid-liquid systems. Kacker et al., (2017) reported an optimal value of five however several industrial studies have demonstrated that significantly higher values of  $\psi$  are required to ensure solids suspension (Agnew et al., 2017; Briggs et al., 2015; Jiang and Ni, 2019; Peña et al., 2017; Zhao et al., 2014); this is further discussed in section 3.2. This highlights that recommended conditions to minimize axial dispersion in single-phase systems may not always be the best choice for multi-phase systems where other process objectives (e.g., solids suspension) may be dominant.

Another characteristic of solid-liquid flows in OBRs is that the solid phase typically has a longer mean residence time than the liquid phase (Ejim et al., 2017). This may be explained by the presence of fluid recirculation loops in the baffle region, where particles can be retained for a longer time than the liquid. The free baffle area,  $\alpha$ , has also been identified as a dominant design parameter in controlling the back-mixing of solids and particle suspension; small values of  $\alpha$  have been found to minimise axial dispersion and increase the mean residence time of particles in the reactor (Ejim et al., 2017; Kacker et al., 2017), which is certainly due to increased transverse velocities. Recently Jimeno et al. (2021) modelled solid-liquid fluid flow in a continuous OBR by coupling a primary Eulerian liquid phase with a secondary discrete Lagrangian phase consisting of solid particles. The results are in agreement with the axial dispersion coefficient and mean residence time results of Ejim et al. (2017) and Kacker et al. (2017). This work allows a better understanding of liquid-solid suspensions, which has previously been limited to empirical correlations obtained from single phase studies.

The impact of baffle geometry on solids suspension has been investigated very little. Reis et al. (2005) showed that OBRs with smooth constrictions require lower oscillation amplitudes that are 50% lower than those required with the sharp-edged orifice baffles for the full suspension of solids. This difference in performance may be due to the creation of poorly mixed zones in the vicinity of sharp-edged orifice baffles (Reis et al., 2005).

#### **3.1.7.4 Gas-Liquid-Solid systems**

A limited number of studies on gas–liquid–solid systems in OBRs are found in the literature. The use of a pulsed baffled tube photochemical reactor has been demonstrated for three-phase heterogeneous catalysed photo-reactions and has shown good performance due to the effective solid handling capacity of this reactor type (Fabiya and Skelton, 2000, 1999). Navarro-Fuentes et al. (2019b, 2019a) carried out catalytic hydrogenation of alkynol to alkenol in an OBR and found that due to the enhanced multiphase mixing and mass transfer, the OBR consumes five times less power, provides more than two times higher  $H_2$  efficiency and 50% lower residence time to achieve the same reaction performance obtained in a commercial STR.

The influence of the solid phase on the gas-liquid mass transfer, hold-up, mean bubble size and bubble distribution have been studied by Ferreira et al. (2017). The presence of solids did not show any significant influence on the Sauter mean diameter ( $d_{32}$ ) or the mass transfer coefficient ( $k_L a$ ) for all operating conditions tested in the study. Although in bubble columns and airlifts, the presence of solids has shown to lead to a decrease in  $k_L a$  (Mena et al., 2005). Indeed, the presence of solids was found to decrease the bubble rise velocity and the bubbles then became trapped in each inter baffle compartment of the OBR, leading to an increase in the gas hold-up and specific interfacial area. It would be expected that this results in increased mass transfer, however, the authors postulate that the solids reduce the renewal rate of the liquid film at the bubble interface, thereby decreasing the liquid-side mass transfer coefficient,  $k_L$  and counter-balancing the possible increase in  $k_L a$  from the increase in specific interfacial area. The understanding of gas-liquid-solid systems is still challenging, and it is a promising area for different industrial applications, such as multiphase bioreactors and catalytic reactions.

### 3.2 Applications and industrial processes

The advantages offered by OBRs (e.g., controlled mixing, which is independent of the bulk flow and allows effective mixing with longer residence times, as well as enhanced multi-phase mixing, heat and mass transfer) has made this reactor type attractive for applications in several industrial sectors, including the polymers industry, biofuels production, chemical industry, pharmaceutical industry and bioprocesses. Table 6 summarizes some industrial examples reported in the literature of reactions and processes carried out in OBRs.

OBRs used in industrial processes are typically manufactured in borosilicate glass, polymers (e.g. poly(methyl methacrylate) and polyethylene) or 316L stainless steel. Depending on the manufacturing material, the OBR can handle process conditions between  $-20$  and  $200^{\circ}\text{C}$  (for stainless steel) and below  $25\text{ bar}^1$  (for the NiTech® OBR), with jacket pressures of  $0 - 1$  bar. Commercial OBRs have different lengths, depending on the required residence time and pressure drop limitations; lengths are typically in the range  $1 - 20$  m. Stonestreet and Harvey (2002) studied different cases to illustrate the mixing design for industrial-scale OBRs, based on lab-scale studies. For the same production rate ( $2.3$  tonnes/hr), smaller length-to-diameter designs with lower power density requirements are obtained for the OBR compared with a tubular reactor. This is possible due to the characteristic recirculating flow of the OBR, which allows good mixing performance for low net velocities (and therefore long residence times) with smaller length-to-diameter ratio tube when compared with conventional tubular reactors (Harvey et al., 2003). These capabilities can be observed in Figure 8 where it can be seen that the length-to-diameter ratio of the OBR is two orders of magnitude lower than that for a tubular reactor for the same production rate, thereby resulting in a much more compact design.

---

<sup>1</sup> <https://www.nitechsolutions.co.uk/products/> (accessed March 11, 2020)

### Power density vs. z/D ratio: Oscillatory Flow Reactor and Tubular reactor

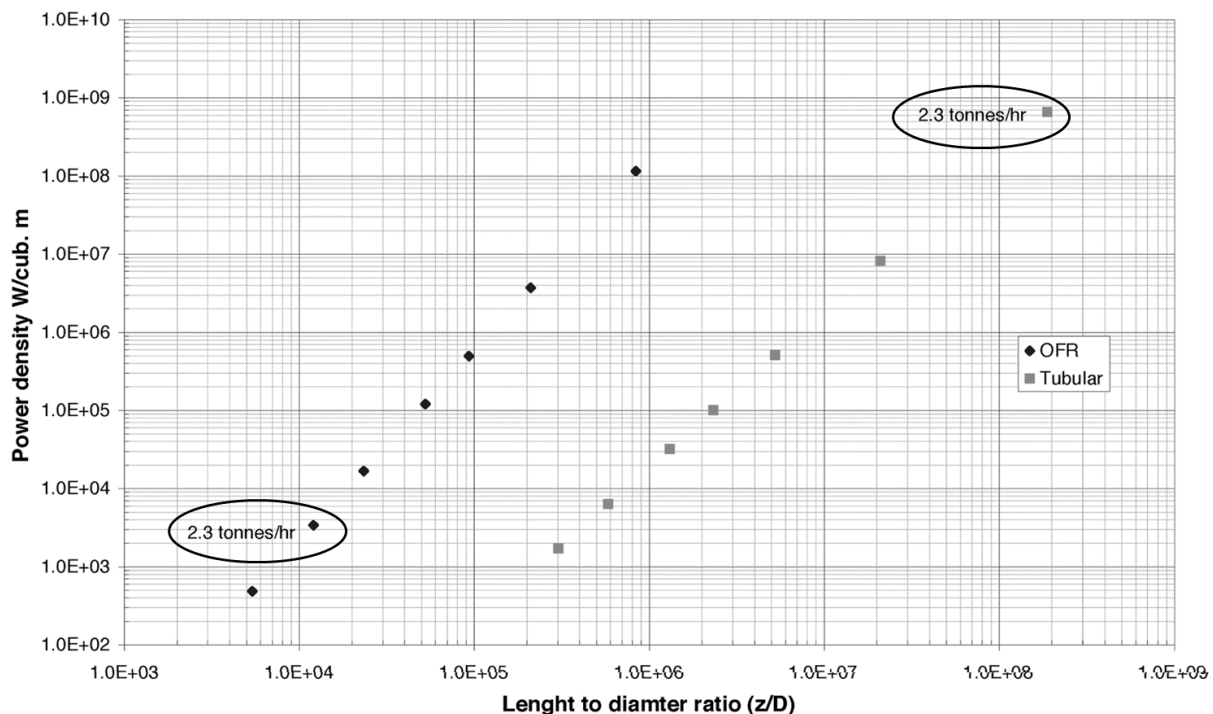


Figure 8: Comparison of power density and length-to-diameter ratio for OFRs and a turbulent flow tubular reactor (Stonestreet and Harvey, 2002).

OFRs in both batch and continuous modes have often been used for industrial crystallization processes (particularly for cooling and anti-solvent crystallization) due to the good temperature control (Ni and Liao, 2008) and mixing between the solvent and antisolvent (Brown and Ni, 2011). Due to the oscillatory flow, OFR crystallizers have been shown to provide high purity crystals (Caldeira and Ni, 2009; McLachlan and Ni, 2016; Zhao et al., 2014), smaller crystals and narrow crystal size distributions (Cruz et al., 2016; Peña et al., 2017; Siddique et al., 2015), when compared with STRs. They also ensure adequate crystal suspension to prevent blockage from occurring (Brown et al., 2015). Furthermore, the presence of the net flow decreases the nucleation induction time due to an increase in the average shear rate (Yang et al., 2015). OFR crystallizers are, nevertheless, less well suited to evaporative and fast reactive crystallizations. As discussed in Section 3.1.3, mixing-dependent applications, such as fast reactive crystallization, are difficult to perform in OFRs due to the difficulty in providing fast micromixing conditions. This can affect the correct nucleation and growth of the crystals, leading to a decrease in selectivity and/or crystal quality, altered product properties and the formation of undesired by-products, thereby requiring high purification costs. Many continuous crystallization processes in oscillatory baffled reactors have been operated with velocity ratios,  $\psi$ , that exceed the upper limit of the recommended range to ensure plug flow operation (i.e.  $2 < \psi < 4$ ,

(Stonestreet and Van Der Veecken, 1999));  $\psi = 82$  is the maximum value found in the literature. Such high velocity ratios are required to ensure solid suspension, as well as uniform particle size and distribution, however they do not necessarily provide plug flow conditions (Agnew et al., 2017; Briggs et al., 2015; Jiang and Ni, 2019; Peña et al., 2017; Zhao et al., 2014). This trend has also been observed for enzymatic hydrolysis with high solid processing, operating with  $\psi$  values between 24 and 42 (Muster-Slawitsch et al., 2020). This highlights that the use of the recommended value of  $\psi$ , as defined for single liquid systems, does not necessarily guarantee effective mixing or adequate process performance for complex multiphase applications.

Production of bio-sourced fuels is a field in which there has been increasing interest over recent years and biodiesel, biobutanol and bioethanol have successfully been produced in OBRs (Hamzah et al., 2012; Ikwebe and Harvey, 2011; Masngut and Harvey, 2012; Phan et al., 2012; Takriff et al., 2009). Biodiesel production is a slow liquid-liquid mass transfer limited reaction and OBRs provide good liquid-liquid contacting and mass transfer, as well as long residence times in compact geometries, which makes them particularly well adapted to such reactions. Among the different designs, the smooth constriction geometry has shown to produce the highest biodiesel content (82%), compared with the wire wool baffle and the sharp edge helical with central rod baffle (74 – 76%). Indeed, the smooth constriction baffle geometry allows stable conversion rates in shorter times and better process performance, thanks to its capability to reach steady state in shorter times (33% faster than the other baffled geometries mentioned above) (Harvey et al., 2003; Mazubert et al., 2014; Phan et al., 2012). The low-shear and good mixing quality offered by OBRs are also well suited to the production of biobutanol and bioethanol, which are made principally by the fermentative action of microorganisms. Such liquid-liquid reactions have typically been carried out with higher velocity ratios  $\psi$  than the recommended range of 2-4 for plug flow in single phase systems ( $\psi = 519$  is the maximum value found in the literature); higher values of  $\psi$  are required in order to ensure adequate liquid-liquid dispersion (Al-Saadi et al., 2019; Mazubert et al., 2015; Phan et al., 2012). Indeed, in liquid-liquid dispersions and reactions, the operating conditions may be chosen such that the oscillatory flow dominates over the net flow, and to ensure the required droplets size and distribution in addition to long residence time, rather than to favour plug flow. Lobry et al. (2014) obtained smaller droplet sizes in a vinyl acetate suspension polymerization due to the shearing action of the oscillatory flow when operating with  $\psi$  values of 12 and 16, which are an order of magnitude greater than the recommended velocity ratio range for plug flow. In some cases, the operating conditions do not follow the recommended range due to size restrictions of the reactor (Harvey et al., 2003), as often occurs in industry.

Recently, the biotechnology company Genzyme (now Sanofi) have improved their new API production via a three-phase reaction on the scale of multi-hundred tons using oscillatory baffled reactors provided by the company NiTech® Solutions, for a process certified by the FDA. The process time in the OBR is 40 times faster than the batch process, and results in higher quality product, reduced maintenance and controlled throughput, leading to a zero-rejection rate for the reaction step<sup>2</sup>. Whilst information on the physical phenomena and the specific reasons for the improved performance in the NiTech® OBR is not detailed in the report, it is expected that the enhanced performance is due to enhanced heat and mass transfer in the three-phase reactive system.

In recent years, many companies have started to incorporate the oscillatory baffled reactor technology from NiTech® Solutions in their processes. Corning Incorporated demonstrated continuous flow chemical manufacturing that integrates the Corning® Advanced-Flow™ reactor and the NiTech® continuous crystallizer with Alconbury Weston Limited continuous filtration equipment<sup>3</sup>. Croda Europe, along with NiTech® Solutions, the Centre for Process Innovation (CPI) and the University of Cambridge's Institute for Manufacturing have also been working on a collaborative project to develop novel methods for continuous production of surfactants<sup>4</sup> to reduce operational and capital costs, increase process sustainability and maintain product quality. SAS PIVERT, an industrial group specialized in agricultural, chemical, and food & feed sectors, has recently acquired a NiTech® COBR DN15 crystalliser/reactor unit for the production of chemical products and energy from oil seed biomass<sup>5</sup>.

The Centre of Excellence for Anaerobic Digestion at the University of New South Wales (USW) has been evaluating the feasibility and efficiency of C1 gas bio-conversion (methane) for energy production and storage using a Nitech® OBR DN60 crystalliser/reactor and comparing it with CSTRs and Liquid Recirculation Reactors (LRR). Methane is synthesised using a patented microbe culture from waste carbon dioxide reacted with hydrogen. Under standardised conditions, the OBR achieved the highest conversion efficiency with 75%, the CSTR 66% and the LLR was ruled out due to insufficient gas flow<sup>6</sup>. The hydrogenation capabilities of the OBR can also be applied in the food

<sup>2</sup> <https://www.nitechsolutions.co.uk/wp-content/uploads/2014/03/HW-case-study-Nov13.pdf> (accessed February 17, 2020)

<sup>3</sup> <https://www.nitechsolutions.co.uk/wp-content/uploads/2015/07/Corning-press-release-Jun15-final.pdf> (accessed March 11, 2020)

<sup>4</sup> <https://www.nitechsolutions.co.uk/wp-content/uploads/2016/02/Newsletter-Feb16.pdf> (accessed March 11, 2020)

<sup>5</sup> <https://www.nitechsolutions.co.uk/nitech-units-to-be-used-in-biotech-research> (accessed March 11, 2020)

<sup>6</sup> <https://www.nitechsolutions.co.uk/market-sectors/biotechnology/university-of-south-wales-case-study/> (accessed March 11, 2020)

industry, especially for processing vegetable oils, where hydrogen changes liquid vegetable oil to a semi-solid or solid fat, and stabilises the oil, thereby preventing its oxidation. In summary, all these practical cases demonstrate that the OBR technology is a viable choice for process intensification of a range of industrial applications. Nevertheless, the operating parameters of the OBR are very often adjusted to the specific application empirically since the existing design guidelines are not robust.

Table 6: Examples of OBR applications.

<b>Reaction / Process</b>	<b>References</b>
Acetylation	(Zheng et al., 2018)
Protein refolding	(Lee et al., 2002, 2001)
Hydrogenation	(Navarro-Fuentes et al., 2019a, 2019b)
Fermentation	(Yussof et al., 2018)
Flocculation	(Gao et al., 1998; Ni et al., 2001a)
Enzymatic reactions	(Abbott et al., 2014b; Ikwebe and Harvey, 2015)
Polymerisation	(Lobry et al., 2014; Ni et al., 1999; Ni et al., 2001b)
Transesterification	(Al-Saadi et al., 2019; Koh et al., 2014; Mazubert et al., 2014, 2013; Soufi et al., 2017)
Solid acid catalysed esterification	(Eze et al., 2017, 2013)
Microalgae culture	(Abbott et al., 2015)
Flotation	(Anderson et al., 2009)
Hydrate formation	(Brown and Ni, 2010)
Synthesis of metal-organic frameworks	(Laybourn et al., 2019)
Photo-oxidation	(Fabiya and Skelton, 1999; Gao et al., 2003)
Ozonation	(Lucas et al., 2016)
Mitigation and wax deposition	(Ismail et al., 2006)
Saponification	(Harvey et al., 2001)
Biofuel production	(Harvey et al., 2003; Kefas et al., 2019; Masngut et al., 2010)
Oil droplet breakage	(Mignard et al., 2006, 2004)
Crystallization / Precipitation	(Briggs et al., 2015; Brown et al., 2015; Castro et al., 2013; Kacker et al., 2017; McLachlan and Ni, 2016; Raval et al., 2020; Siddique et al., 2015)
Cross flow filtration	(Horie et al., 2018)



### 3.3 Further discussion on the limitations of recommended operating conditions

The oscillatory baffled reactor, in both batch and continuous operation, has already been proven to enhance mixing in single and multiphase systems, mass and heat transfer, as well as to use less energy than conventional reactors, like STRs. COBRs have successfully been applied in many different industrial applications due to the possibility of obtaining good mixing quality independently of net flow, even under slow flow conditions when long residence times are required. In the literature, a number of guidelines for 'optimal' operating conditions have been proposed and have been widely adopted by researchers and users of OBRs over the last decades. However, most of these guidelines have been based on qualitative flow observations and the analysis of plug flow behaviour of the reactor for single-phase systems (water or similar). Unfortunately, these guidelines may not be so well adapted when applied to more complex systems with multi-physics and multiple phases, and therefore many industrial applications. Industrial processes are also confronted with multiple constraints related to pressure drop, residence time, materials compatibility, heat transfer, reaction yield/selectivity/conversion, which may require different oscillatory and flow conditions.

For single orifice OBRs, Stonestreet and Van Der Veecken (1999) showed that for systems where  $Re_{net} > 250$ , the influence of the oscillatory flow becomes disadvantageous in single orifice OBRs. Indeed, when the net flow is too high, the characteristic flow pattern created by oscillations is overridden and the mixing quality and efficiency is decreased. High net flows also lead to shorter residence times, and therefore increased reactor lengths may be required to achieve sufficient reaction conversion but in detriment of pressure drop. Additionally, Stonestreet and Harvey (2002) recommended a minimum net Reynolds number of 50 to achieve convection. However, these recommended limits  $50 < Re_{net} < 250$  may not necessarily be easy to achieve, especially for low viscosity applications. Processes using high viscosity liquids or where the viscosity increases as the reaction progress (like some polymerisations) may not be so limited by these guidelines, however the latter case may be one of the most challenging situations since different flows and reactor designs may be required during the process. Hence, depending on the application (i.e., the fluids used and the process objectives), the most appropriate and practical ranges of  $Re_{net}$  may vary. A modification of the reactor diameter may be a solution to achieve a desired  $Re_{net}$  when working with viscous fluids or when an increase in the flow rate is not practical; however, in some cases, this kind of modification cannot always be made and could require an additional reactor. An analysis of operating and capital expenses therefore must be carried out in order to choose the most adapted solution.

As it has been discussed throughout this paper, it appears that the recommended and ‘optimal’ operating conditions as presented in the literature may not always be well suited to the application in question. Indeed, the most appropriate operating conditions may depend on the process objective and the relevant parameters used to characterize the process performance; these will depend on the nature and the physics of the application. In some cases, when operating conditions present opposing effects on the reactor performance, a compromise may need to be established to obtain the best solution possible, based on the limiting phenomenon or the product-controlling phenomenon in the process. Some examples of conflicting operating conditions can be found in the literature. Fabiyi and Skelton (1999) performed a photo-catalysed mineralization of methylene blue in a pulsed baffled tube. The mass transfer (adsorption) enhanced with an increase of the mixing intensity (i.e., increase in the oscillatory conditions). However, the reaction rate did not improve with this increase in mass transfer. This was because an increase in the oscillatory Reynolds number increased the apparent scattering centres (particles that absorb light energy and re-emit it in different directions with different intensities) within the reactor since the uniformity of particle concentration was modified. An increase in the particle concentration at constant concentration of the absorbing species produces an increase in the optical thickness and an increase in the scattering albedo (i.e., ratio of scattering efficiency to total extinction efficiency), thereby leading to a decrease in the average reaction rate with respect to the case with no scattering.

#### **4 Conclusions and perspectives**

This review of the state of art presents an update of the oscillatory baffled reactor technology, for both, batch and continuous operations. The key geometrical parameters and dimensionless groups in the design of the reactor, and the most used ranges of operating parameters in the literature have been presented, along with the various baffle geometries that have been investigated to date. These geometries are easily adopted for different applications by only adjusting the operating conditions depending on the final process objective.

Flow performance studies carried out to characterize OBRs as a function of the application and the process type have been highlighted. OBR technology has proven to enhance mixing, heat and mass transfer, as well as gas-liquid and liquid-liquid dispersion and solid suspensions. Due to this, OBRs have been used for many single phase and multiphase applications, such as polymers, biofuels, chemical reactions, pharmaceutical and bioprocesses. More recent studies have demonstrated that OBRs can achieve good gas-liquid mass transfer with the presence of a solid catalyst, extending the

industrial applications where oscillatory baffled reactor is already implemented, like multiphase bioreactors and catalytic reactions. Despite these successful demonstrations, the implementation of OBRs is still challenging for some applications, such as fast reactive crystallization, processes employing highly viscous fluids or solids suspension with high particle concentration. This is due to geometrical restrictions of the reactor, as well as the lack of studies and understanding of the associated phenomena within the OBR.

An important aspect of the recommended and optimal operating conditions widely used in the literature has been discussed. Many characterization studies limit their operating conditions to achieve and maintain plug flow in the reactor. However, parameters other than plug flow behaviour, such as conversion rate, dispersion, macromixing, micromixing, particle size and distribution, etc. may also be a priority depending on the process objectives. The choice of the most convenient method to characterize OBR performance, along with the optimal operating parameters, will therefore depend on the nature and final goal of the process.

## 5 Nomenclature

$A$	OBR cross-sectional area ( $\text{m}^2$ )
$C$	species concentration ( $\text{kg m}^{-3}$ )
$C_D$	orifice discharge coefficient (-)
$C_p$	fluid specific heat capacity ( $\text{J kg}^{-1} \text{K}^{-1}$ )
$D$	OBR diameter (m)
$d$	OBR orifice diameter (m)
$D_{ax}$	axial dispersion coefficient ( $\text{m}^2 \text{s}^{-1}$ )
$D_h$	hydraulic diameter (m)
$d_{32}$	Sauter mean diameter (m)
$d_e$	equivalent diameter (m)
$d_{v,0.5}$	mean particle size (m)
$f$	oscillation frequency (Hz)
$h_{OBR}$	OBR-side transfer coefficient ( $\text{W m}^{-2} \text{K}^{-1}$ )

$k$	thermal conductivity of the process fluid ( $\text{W m}^{-1} \text{K}^{-1}$ )
$k_L$	liquid-side mass transfer coefficient ( $\text{m s}^{-1}$ )
$k_L a$	volumetric mass transfer coefficient ( $\text{s}^{-1}$ )
$l$	mixing length (m)
$l^*$	mixing length proposed by Jimeno et al. (2018b) (m)
$l_b$	distance between baffles (m)
$l_b^{opt}$	optimum distance between baffles (m)
$L$	reactor length (m)
$n$	number of baffles (-)
$Nu$	Nusselt number (-)
$Pr$	Prandtl number $\left( C_p \mu / k \right)$ (-)
$P/V$	power density ( $\text{W m}^{-3}$ )
$(P/V)^*$	dimensionless power density (-)
$Pe$	Péclet number (-)
$R$	radius of reactor (m)
$R_{VA}$	axial to radial velocity ratio, weighted by area (-)
$R_{VV}$	axial to radial velocity ratio, weighted by volume (-)
$Re_{net}$	net flow Reynolds number (-)
$Re_o$	oscillatory Reynolds number (-)
$Re_{oh}$	hydrodynamic oscillatory Reynolds number (-)
$Re_T$	total Reynolds number proposed by Jimeno et al. (2018b) (-)
$r$	radial coordinate (m)
$r_n$	radial number (-)
$S_n$	swirl number (-)
$St$	Strouhal number (-)

$t$	time (s)
$\bar{u}$	mean velocity ( $\text{m s}^{-1}$ )
$u_{i,z}$	axial velocity in computational cell $i$ ( $\text{m s}^{-1}$ )
$u_{i,r}$	transverse or radial velocity in computational cell $i$ ( $\text{m s}^{-1}$ )
$u_{net}$	net velocity ( $\text{m s}^{-1}$ )
$u_x, u_y, u_z$	velocity components ( $\text{m s}^{-1}$ )
$V$	volume ( $\text{m}^3$ )
$v_r$	radial velocity ( $\text{m s}^{-1}$ )
$v_z$	axial velocity (cylindrical coordinate) ( $\text{m s}^{-1}$ )
$v_\theta$	tangential velocity ( $\text{m s}^{-1}$ )
$x_o$	center-to peak oscillation amplitude (m)
$We_h$	hydrodynamic Weber number (-)
$We_s$	Weber number (-)
$x, y, z$	Cartesian coordinates (m)

### Greek symbols

$\alpha$	dimensionless free baffle area $\left(\frac{d}{D}\right)^2$ (-)
$\beta$	optimal baffle spacing ratio (-)
$\delta$	baffle thickness (m)
$\lambda$	coefficient of thermal performance by Ahmed et al. (2018a) (-)
$\mu$	dynamic viscosity (Pa.s)
$\rho$	fluid density ( $\text{kg m}^{-3}$ )
$\varphi$	correction factor (-)
$\psi$	velocity ratio (-)
$\omega$	oscillation angular frequency ( $\text{rad s}^{-1}$ )

## 6 Declaration of competing interest

The authors declare that they have no know competing financial interests or personal relationships that could have appeared to influence the work reported in this paper.

## 7 Acknowledgements

The authors acknowledge the Mexican Council of Science and Technology (CONACYT México), the French Ministry of Higher Education, Research and Innovation, and Toulouse INP for diverse support and funding.

## 8 References

- Abbott, M.S.R., Brain, C.M., Harvey, A.P., Morrison, M.I., Valente Perez, G., 2015. Liquid culture of microalgae in a photobioreactor (PBR) based on oscillatory baffled reactor (OBR) technology – A feasibility study. *Chem. Eng. Sci.* 138, 315–323. <https://doi.org/10.1016/j.ces.2015.07.045>
- Abbott, M.S.R., Harvey, A.P., Morrison, M.I., 2014a. Rapid determination of the residence time distribution (RTD) function in an oscillatory baffled reactor (OBR) using a design of experiments (DoE) approach. *Int. J. Chem. React. Eng.* 12, 575–586. <https://doi.org/10.1515/ijcre-2014-0040>
- Abbott, M.S.R., Harvey, A.P., Valente Perez, G., Theodorou, M.K., 2013. Biological processing in oscillatory baffled reactors: operation, advantages and potential. *Interface Focus* 3, 20120036. <https://doi.org/10.1098/rsfs.2012.0036>
- Abbott, M.S.R., Valente Perez, G., Harvey, A.P., Theodorou, M.K., 2014b. Reduced power consumption compared to a traditional stirred tank reactor (STR) for enzymatic saccharification of alpha-cellulose using oscillatory baffled reactor (OBR) technology. *Chem. Eng. Res. Des.* 92, 1969–1975. <https://doi.org/10.1016/j.cherd.2014.01.020>
- Abdul, M.A., Phan, A.N., Harvey, A.P., 2020. Intensification of epoxidation of vegetable oils using a continuous mesoscale oscillatory baffled reactor. *J. Adv. Manuf. Process.* 2, 1–12. <https://doi.org/10.1002/amp2.10041>
- Agnew, L.R., McGlone, T., Wheatcroft, H.P., Robertson, A., Parsons, A.R., Wilson, C.C., 2017. Continuous crystallization of paracetamol (acetaminophen) form II: selective access to a metastable solid form. *Cryst. Growth Des.* 17, 2418–2427. <https://doi.org/10.1021/acs.cgd.6b01831>
- Ahmed, S.M.R., Law, R., Phan, A.N., Harvey, A.P., 2018a. Thermal performance of meso-scale oscillatory baffled reactors. *Chem. Eng. Process. - Process Intensif.* 132, 25–33. <https://doi.org/10.1016/j.cep.2018.08.009>

- Ahmed, S.M.R., Phan, A.N., Harvey, A.P., 2018b. Mass transfer enhancement as a function of oscillatory baffled reactor design. *Chem. Eng. Process. - Process Intensif.* 130, 229–239. <https://doi.org/10.1016/j.cep.2018.06.016>
- Ahmed, S.M.R., Phan, A.N., Harvey, A.P., 2017. Scale-up of oscillatory helical baffled reactors based on residence time distribution. *Chem. Eng. Technol.* 40, 907–914. <https://doi.org/10.1002/ceat.201600480>
- Al-Abduly, A., Christensen, P., Harvey, A., Zahng, K., 2014. Characterization and optimization of an oscillatory baffled reactor (OBR) for ozone-water mass transfer. *Chem. Eng. Process. Process Intensif.* 84, 82–89. <https://doi.org/10.1016/j.cep.2014.03.015>
- Al-Khani, S.D., Gourdon, C., Casamatta, G., 1988. Simulation of hydrodynamics and mass transfer of a disks and rings pulsed column. *Ind. Eng. Chem. Res.* 27, 329–333. <https://doi.org/10.1021/ie00074a020>
- Al-Saadi, L.S., Alegría, A., Eze, V.C., Harvey, A.P., 2019. Rapid screening of an acid-catalyzed triglyceride transesterification in a mesoscale reactor. *Chem. Eng. Technol.* 42, 539–548. <https://doi.org/10.1002/ceat.201800203>
- Alberini, F., Simmons, M.J.H., Ingram, A., Stitt, E.H., 2014. Use of an areal distribution of mixing intensity to describe blending of non-newtonian fluids in a Kenics KM static mixer using PLIF. *AIChE J.* 60, 332–342. <https://doi.org/10.1016/j.ces.2014.03.022>
- Amokrane, A., Charton, S., Lamadie, F., Paisant, J.F., Puel, F., 2014. Single-phase flow in a pulsed column: particle image velocimetry validation of a CFD based model. *Chem. Eng. Sci.* 114, 40–50. <https://doi.org/10.1016/j.ces.2014.04.003>
- Anderson, C.J., Harris, M.C., Deglon, D.A., 2009. Flotation in a novel oscillatory baffled column. *Miner. Eng.* 22, 1079–1087. <https://doi.org/10.1016/j.mineng.2009.04.007>
- Angelov, G., Gourdon, C., 2012. Pressure drop in pulsed extraction columns with internals of discs and doughnuts. *Chem. Eng. Res. Des.* 90, 877–883. <https://doi.org/10.1016/j.cherd.2011.10.011>
- Angelov, G., Journe, E., Line, A., Gourdon, C., 1990. Simulation of the flow patterns in a disc and doughnut column. *Chem. Eng. J.* 45, 87–97. [https://doi.org/10.1016/0300-9467\(90\)80031-7](https://doi.org/10.1016/0300-9467(90)80031-7)
- Avila, M., Fletcher, D.F., Poux, M., Xuereb, C., Aubin, J., 2020a. Mixing performance in continuous oscillatory baffled reactors. *Chem. Eng. Sci.* 219, 115600. <https://doi.org/10.1016/j.ces.2020.115600>
- Avila, M., Fletcher, D.F., Poux, M., Xuereb, C., Aubin, J., 2020b. Predicting power consumption in continuous oscillatory baffled reactors. *Chem. Eng. Sci.* 212, 115310. <https://doi.org/10.1016/j.ces.2019.115310>
- Baird, M.H.I., Stonestreet, P., 1995. Energy dissipation in oscillatory flow within a baffled tube. *Trans IChemE* 73(A), 503–511.
- Baldyga, J., Pohorecki, R., 1995. Turbulent micromixing in chemical reactors - a review. *Chem. Eng. J.* 58, 183–195. [https://doi.org/10.1016/0923-0467\(95\)02982-6](https://doi.org/10.1016/0923-0467(95)02982-6)

- Bianchi, P., Williams, J.D., Kappe, C.O., 2020. Oscillatory flow reactors for synthetic chemistry applications. *J. Flow Chem.* 10, 475–490. <https://doi.org/10.1007/s41981-020-00105-6>
- Briggs, N.E.B., Schacht, U., Raval, V., McGlone, T., Sefcik, J., Florence, A.J., 2015. Seeded crystallization of  $\beta$ -L-glutamic acid in a continuous oscillatory baffled crystallizer. *Org. Process Res. Dev.* 19, 1903–1911. <https://doi.org/10.1021/acs.oprd.5b00206>
- Brown, C.J., Adelakun, J.A., Ni, X., 2015. Characterization and modelling of antisolvent crystallization of salicylic acid in a continuous oscillatory baffled crystallizer. *Chem. Eng. Process. Process Intensif.* 97, 180–186. <https://doi.org/10.1016/j.cep.2015.04.012>
- Brown, C.J., Ni, X., 2011. Evaluation of growth kinetics of antisolvent crystallization of paracetamol in an oscillatory baffled crystallizer utilizing video imaging. *Cryst. Growth Des.* 11, 3994–4000. <https://doi.org/10.1021/cg200560b>
- Brown, C.J., Ni, X., 2010. Evaluation of rate of cyclopentane hydrate formation in an oscillatory baffled column using laser induced fluorescence and energy balance. *Chem. Eng. J.* 157, 131–139. <https://doi.org/10.1016/j.cej.2009.11.019>
- Brunold, C.R., Hunns, J.C.B., Mackley, M.R., Thompson, J.W., 1989. Experimental observations on flow patterns and energy losses for oscillatory flow in ducts containing sharp edges. *Chem. Eng. Sci.* 44, 1227–1244. [https://doi.org/10.1016/0009-2509\(89\)87022-8](https://doi.org/10.1016/0009-2509(89)87022-8)
- Caldeira, R., Ni, X., 2009. Evaluation and establishment of a cleaning protocol for the production of vanilic sodium and aspirin using a continuous oscillatory baffled reactor. *Org. Process Res. Dev.* 13, 1080–1087. <https://doi.org/10.1021/op900120h>
- Callahan, C.J., Ni, X., 2014. An investigation into the effect of mixing on the secondary nucleation of sodium chlorate in a stirred tank and an oscillatory baffled crystallizer. *CrystEngComm* 16, 690–697. <https://doi.org/10.1039/C3CE41467A>
- Castro, F., Ferreira, A., Rocha, F., Vicente, A., Teixeira, J.A., 2013. Continuous-flow precipitation of hydroxyapatite at 37 °C in a meso oscillatory flow reactor. *Ind. Eng. Chem. Res.* 52, 9816–9821. <https://doi.org/10.1021/ie400710b>
- Cruz, P., Rocha, F., Ferreira, A., 2016. Effect of operating conditions on batch and continuous paracetamol crystallization in an oscillatory flow mesoreactor. *CrystEngComm* 18, 9113–9121. <https://doi.org/10.1039/c6ce01648k>
- Dickens, A.W., Mackley, M.R., Williams, H.R., 1989. Experimental residence time distribution measurements for unsteady flow in baffled tubes. *Chem. Eng. Sci.* 44, 1471–1479. [https://doi.org/10.1016/0009-2509\(89\)80023-5](https://doi.org/10.1016/0009-2509(89)80023-5)
- Ejim, L.N., Yerdelen, S., Mcglone, T., Onyemelukwe, I., Johnston, B., Florence, A.J., Reis, N., 2017. A factorial approach to understanding the effect of inner geometry of baffled meso-scale tubes on solids suspension and axial dispersion in continuous, oscillatory liquid-solid plug flows. *Chem. Eng. J.* 308, 669–682. <https://doi.org/10.1016/j.cej.2016.09.013>
- Eze, V.C., Fisher, J.C., Phan, A.N., Harvey, A.P., 2017. Intensification of carboxylic acid esterification using a solid catalyst in a mesoscale oscillatory baffled reactor platform. *Chem.*



Eng. J. 322, 205–214. <https://doi.org/10.1016/j.cej.2017.04.038>

- Eze, V.C., Phan, A.N., Pirez, C., Harvey, A.P., Lee, A.F., Wilson, K., 2013. Heterogeneous catalysis in an oscillatory baffled flow reactor. *Catal. Sci. Technol.* 3, 2373. <https://doi.org/10.1039/c3cy00282a>
- Fabiyi, M.E., Skelton, R.L., 2000. Photocatalytic mineralisation of methylene blue using buoyant TiO<sub>2</sub>-coated polystyrene beads. *J. Photochem. Photobiol. A Chem.* 132, 121–128. [https://doi.org/10.1016/S1010-6030\(99\)00250-6](https://doi.org/10.1016/S1010-6030(99)00250-6)
- Fabiyi, M.E., Skelton, R.L., 1999. The application of oscillatory flow mixing to photocatalytic wet oxidation. *J. Photochem. Photobiol. A Chem.* 129, 17–24. [https://doi.org/10.1016/S1010-6030\(99\)00177-X](https://doi.org/10.1016/S1010-6030(99)00177-X)
- Ferreira, A., Adesite, P.O., Teixeira, J.A., Rocha, F., 2017. Effect of solids on O<sub>2</sub> mass transfer in an oscillatory flow reactor provided with smooth periodic constrictions. *Chem. Eng. Sci.* 170, 400–409. <https://doi.org/10.1016/j.ces.2016.12.067>
- Ferreira, A., Teixeira, J.A., Rocha, F., 2015. O<sub>2</sub> mass transfer in an oscillatory flow reactor provided with smooth periodic constrictions. Individual characterization of k<sub>L</sub> and a. *Chem. Eng. J.* 262, 499–508. <https://doi.org/10.1016/j.cej.2014.09.125>
- Fitch, A.W., Jian, H., Ni, X., 2005. An investigation of the effect of viscosity on mixing in an oscillatory baffled column using digital particle image velocimetry and computational fluid dynamics simulation. *Chem. Eng. J.* 112, 197–210. <https://doi.org/10.1016/j.cej.2005.07.013>
- Gao, P., Han Ching, W., Herrmann, M., Kwong Chan, C., Yue, P.L., 2003. Photooxidation of a model pollutant in an oscillatory flow reactor with baffles. *Chem. Eng. Sci.* 58, 1013–1020. [https://doi.org/10.1016/S0009-2509\(02\)00642-5](https://doi.org/10.1016/S0009-2509(02)00642-5)
- Gao, S., Ni, X., Cumming, R.H., Greated, C.A., Norman, P., 1998. Experimental investigation of bentonite flocculation in a batch oscillatory baffled column. *Sep. Sci. Technol.* 33, 2143–2157.
- Golding, J.A., Lee, J., 1981. Recovery and separation of cobalt and nickel in a pulsed sieve-plate extraction column. *Ind. Eng. Chem. Process Des. Dev.* 20, 256–261. <https://doi.org/10.1021/i200013a013>
- González-Juárez, D., Herrero-Martín, R., Solano, J.P., 2018. Enhanced heat transfer and power dissipation in oscillatory-flow tubes with circular-orifice baffles: a numerical study. *Appl. Therm. Eng.* 141, 494–502. <https://doi.org/10.1016/j.applthermaleng.2018.05.115>
- González-Juárez, D., Solano, J.P., Herrero-Martín, R., Harvey, A.P., 2017. Residence time distribution in multiorifice baffled tubes: a numerical study. *Chem. Eng. Res. Des.* 118, 259–269. <https://doi.org/10.1016/j.cherd.2016.12.008>
- Gough, P., Ni, X., Symes, K.C., 1997. Experimental flow visualisation in a modified pulsed baffled reactor. *J. Chem. Technol. Biotechnol.* 69, 321–328. [https://doi.org/10.1002/\(SICI\)1097-4660\(199707\)69](https://doi.org/10.1002/(SICI)1097-4660(199707)69)
- Hamzah, A.A., Hasan, N., Takriff, M.S., Kamarudin, S.K., Abdullah, J., Tan, I.M., Sern, W.K., 2012.

Effect of oscillation amplitude on velocity distributions in an oscillatory baffled column (OBC). *Chem. Eng. Res. Des.* 90, 1038–1044. <https://doi.org/10.1016/j.cherd.2011.11.003>

Hartman, R.L., McMullen, J.P., Jensen, K.F., 2011. Deciding whether to go with the flow: evaluating the merits of flow reactors for synthesis. *Angew. Chemie - Int. Ed.* 50, 7502–7519. <https://doi.org/10.1002/anie.201004637>

Harvey, A.P., Mackley, M.R., Seliger, T., 2003. Process intensification of biodiesel production using a continuous oscillatory flow reactor. *J. Chem. Technol. Biotechnol.* 78, 338–341. <https://doi.org/10.1002/jctb.782>

Harvey, A.P., Mackley, M.R., Stonestreet, P., 2001. Operation and optimization of an oscillatory flow continuous reactor. *Ind. Eng. Chem. Res.* 40, 5371–5377. <https://doi.org/10.1021/ie0011223>

Hewgill, M.R., Mackley, M.R., Pandit, A.B., Pannu, S.S., 1993. Enhancement of gas-liquid mass transfer using oscillatory flow in a baffled tube. *Chem. Eng. Sci.* 48, 799–809. [https://doi.org/10.1016/0009-2509\(93\)80145-G](https://doi.org/10.1016/0009-2509(93)80145-G)

Horie, T., Shiota, S., Akagi, T., Ohmura, N., Wang, S., Eze, V., Harvey, A., Hirata, Y., 2018. Intensification of hollow fiber membrane cross-flow filtration by the combination of helical baffle and oscillatory flow. *J. Memb. Sci.* 554, 134–139. <https://doi.org/10.1016/j.memsci.2018.01.058>

Hornung, C.H., Mackley, M.R., 2009. The measurement and characterisation of residence time distributions for laminar liquid flow in plastic microcapillary arrays. *Chem. Eng. Sci.* 64, 3889–3902. <https://doi.org/10.1016/j.ces.2009.05.033>

Ikwebe, J., Harvey, A.P., 2015. Enzymatic saccharification of cellulose: a study of mixing and agitation in an oscillatory baffled reactor and a stirred tank reactor. *Biofuels* 6, 203–208. <https://doi.org/10.1080/17597269.2015.1078560>

Ikwebe, J., Harvey, A.P., 2011. Intensification of bioethanol production by simultaneous saccharification and fermentation (SSF) in an oscillatory baffled reactor (OBR). *World Renew. Energy Congr.* 157, 381–388. <https://doi.org/10.3384/ecp11057381>

Ismail, L., Westacott, R.E., Ni, X., 2006. On the characterisation of wax deposition in an oscillatory baffled device. *J. Chem. Technol. Biotechnol.* 81, 1905–1914. <https://doi.org/https://doi.org/10.1002/jctb.1623>

Jealous, A.C., Johnson, H.F., 1955. Power requirements for pulse generation in pulse columns. *Ind. Eng. Chem.* 47, 1159–1166. <https://doi.org/10.1021/ie50546a021>

Jian, H., Ni, X., 2005. A numerical study on the scale-up behaviour in oscillatory baffled columns. *Chem. Eng. Res. Des.* 83, 1163–1170. <https://doi.org/10.1205/cherd.03312>

Jiang, M., Ni, X., 2019. Reactive crystallization of paracetamol in a continuous oscillatory baffled reactor. *Org. Process Res. Dev.* 23, 882–890. <https://doi.org/10.1021/acs.oprd.8b00446>

Jimeno, G., 2019. Characterisation of solid-liquid flow in a continuous oscillatory baffled reactor

using computational fluid dynamics. PhD Diss. Heriot Watt Univ.

- Jimeno, G., Lee, Y.C., Ni, X., 2021. The effect of particle size on flow in a continuous oscillatory baffled reactor using CFD. *Can. J. Chem. Eng.* 1–14. <https://doi.org/10.1002/cjce.24125>
- Jimeno, G., Lee, Y.C., Ni, X., 2018. On the evaluation of power density models for oscillatory baffled reactors using CFD. *Chem. Eng. Process. - Process Intensif.* 134, 153–162. <https://doi.org/10.1016/J.CEP.2018.11.002>
- Johansen, F.C., 1930. Flow through pipe orifices at low reynolds numbers. *Proc. R. Soc. A Math. Phys. Eng. Sci.* 126, 231–245. <https://doi.org/10.1098/rspa.1930.0004>
- Kacker, R., Regensburg, S.I., Kramer, H.J.M., 2017. Residence time distribution of dispersed liquid and solid phase in a continuous oscillatory flow baffled crystallizer. *Chem. Eng. J.* 317, 413–423. <https://doi.org/10.1016/j.cej.2017.02.007>
- Karr, A.E., 1959. Performance of a reciprocating-plate extraction column. *AIChE J.* 5, 446–452. <https://doi.org/10.1002/aic.690050410>
- Kefas, H.M., Yunus, R., Rashid, U., Taufiq-Yap, Y.H., 2019. Enhanced biodiesel synthesis from palm fatty acid distillate and modified sulfonated glucose catalyst via an oscillation flow reactor system. *J. Environ. Chem. Eng.* 7, 102993. <https://doi.org/10.1016/j.jece.2019.102993>
- Knott, G.F., Mackley, M.R., 1980. On eddy motions near plates and ducts, induced by water waves and periodic flows. *Philos. Trans. R. Soc. London. Ser. A Math. Phys. Sci.* 294, 599–623. <https://doi.org/10.1098/rsta.1980.0070>
- Koh, M.Y., Idaty, T., Ghazi, M., Idris, A., Tinia, T.I., Idris, A., 2014. Synthesis of palm based biolubricant in an oscillatory flow reactor (OFR). *Ind. Crops Prod.* 52, 567–574. <https://doi.org/10.1016/j.indcrop.2013.10.042>
- Kukukova, A., Aubin, J., Kresta, S.M., 2009. A new definition of mixing and segregation: three dimensions of a key process variable. *Chem. Eng. Res. Des.* 87, 633–647. <https://doi.org/10.1016/j.cherd.2009.01.001>
- Kumar, A., Hartland, S., 1988. Prediction of dispersed phase hold-up in pulsed perforated-plate extraction columns. *Chem. Eng. Process.* 23, 41–59. [https://doi.org/10.1016/0255-2701\(88\)87013-2](https://doi.org/10.1016/0255-2701(88)87013-2)
- Laulan, A., 1980. Hydrodynamics and drop splitting in a pulsed disc and ring column. PhD Diss. INP-Toulouse.
- Law, R., Ahmed, S., Tang, N., Phan, A., Harvey, A., 2018. Development of a more robust correlation for predicting heat transfer performance in oscillatory baffled reactors. *Chem. Eng. Process. - Process Intensif.* 125, 133–138. <https://doi.org/10.1016/j.cep.2018.01.016>
- Laybourn, A., López-Fernández, A.M., Thomas-Hillman, I., Katrib, J., Lewis, W., Dodds, C., Harvey, A.P., Kingman, S.W., 2019. Combining continuous flow oscillatory baffled reactors and microwave heating: process intensification and accelerated synthesis of metal-organic frameworks. *Chem. Eng. J.* 356, 170–177. <https://doi.org/10.1016/j.cej.2018.09.011>

- Lee, C.T., Buswell, A.M., Middelberg, A.P.J., 2002. The influence of mixing on lysozyme renaturation during refolding in an oscillatory flow and a stirred-tank reactor. *Chem. Eng. Sci.* 57, 1679–1684. [https://doi.org/10.1016/S0009-2509\(02\)00066-0](https://doi.org/10.1016/S0009-2509(02)00066-0)
- Lee, C.T., Mackley, M.R., Stonestreet, P., Middelberg, A.P.J., 2001. Protein refolding in an oscillatory flow reactor. *Biotechnol. Lett.* 23, 1899–1901. <https://doi.org/10.1023/A:1012734214751>
- Leroy, P., 1991. Study on the pressure drop in pulsed disc and doughnut columns. PhD Diss. INP-Lorraine.
- Levenspiel, O., 2012. Tracer technology: modeling the flow of fluids. Springer, New York. <https://doi.org/10.1007/978-1-4419-8074-8>
- Liu, S., Afacan, A., Masliyah, J.H., 2001. A new pressure drop model for flow-through orifice plates. *Can. J. Chem. Eng.* 79, 100–106. <https://doi.org/10.1002/cjce.5450790115>
- Lobry, E., Gourdon, C., Xuereb, C., Lasuye, T., 2013. Liquid-liquid dispersion in co-current disc and doughnut pulsed column effect of the operating conditions, physical properties and materials parameters. *Chem. Eng. J.* 233, 24–38. <https://doi.org/10.1016/j.cej.2013.08.020>
- Lobry, E., Lasuye, T., Gourdon, C., Xuereb, C., 2014. Liquid-liquid dispersion in a continuous oscillatory baffled reactor - application to suspension polymerization. *Chem. Eng. J.* 259, 505–518. <https://doi.org/10.1016/j.cej.2014.08.014>
- Loudon, C., Tordesillas, A., 1998. The use of the dimensionless Womersley number to characterize the unsteady nature of internal flow. *J. Theor. Biol.* 193, 63–78. <https://doi.org/10.1006/jtbi.1997.0564>
- Lucas, M.S., Reis, N.M., Puma, G.L., 2016. Intensification of ozonation processes in a novel, compact, multi-orifice oscillatory baffled column. *Chem. Eng. J.* 296, 335–339. <https://doi.org/10.1016/j.cej.2016.03.050>
- Mackley, M.R., Ni, X., 1991. Mixing and dispersion in a baffled tube for steady laminar and pulsatile flow. *Chem. Eng. Sci.* 46, 3139–3151. [https://doi.org/10.1016/0009-2509\(91\)85017-R](https://doi.org/10.1016/0009-2509(91)85017-R)
- Mackley, M.R., Smith, K.B., Wise, N.P., 1993. The mixing and separation of particle suspensions using oscillatory flow in baffled tubes. *Trans IChemE* 71, 649–656.
- Mackley, M.R., Stonestreet, P., 1995. Heat transfer and associated energy dissipation for oscillatory flow in baffled tubes. *Chem. Eng. Sci.* 50, 2211–2224.
- Manninen, M., Gorshkova, E., Immonen, K., Ni, X., 2013. Evaluation of axial dispersion and mixing performance in oscillatory baffled reactors using CFD. *J. Chem. Technol. Biotechnol.* 88, 553–562. <https://doi.org/10.1002/jctb.3979>
- Martin, G., 1987. Extraction from viscous polymer solutions. *Chem. Eng. Prog.* 83, 54–55.
- Masngut, N., Harvey, A.P., 2012. Intensification of biobutanol production in batch oscillatory baffled bioreactor. *Procedia Eng.* 42, 1079–1087. <https://doi.org/10.1016/j.proeng.2012.07.499>

- Masngut, N., Harvey, A.P., Ikwebe, J., 2010. Potential uses of oscillatory baffled reactors for biofuel production. *Biofuels* 1, 605–619. <https://doi.org/10.4155/bfs.10.38>
- Mazubert, A., Aubin, J., Elgue, S., Poux, M., 2014. Intensification of waste cooking oil transformation by transesterification and esterification reactions in oscillatory baffled and microstructured reactors for biodiesel production. *Green Process. Synth.* 3, 419–429. <https://doi.org/10.1515/gps-2014-0057>
- Mazubert, A., Crockatt, M., Poux, M., Aubin, J., Roelands, M., 2015. Reactor comparison for the esterification of fatty acids from waste cooking oil. *Chem. Eng. Technol.* 38, 2161–2169. <https://doi.org/10.1002/ceat.201500138>
- Mazubert, A., Fletcher, D.F., Poux, M., Aubin, J., 2016a. Hydrodynamics and mixing in continuous oscillatory flow reactors—Part I: effect of baffle geometry. *Chem. Eng. Process. Process Intensif.* 108, 78–92.
- Mazubert, A., Fletcher, D.F., Poux, M., Aubin, J., 2016b. Hydrodynamics and mixing in continuous oscillatory flow reactors—Part II: characterisation methods. *Chem. Eng. Process. Process Intensif.* 102, 102–116.
- Mazubert, A., Poux, M., Aubin, J., 2013. Intensified processes for FAME production from waste cooking oil: a technological review. *Chem. Eng. J.* 233, 201–223. <https://doi.org/10.1016/j.cej.2013.07.063>
- McDonough, J.R., Ahmed, S.M.R., Phan, A.N., Harvey, A.P., 2019a. The development of helical vortex pairs in oscillatory flows – a numerical and experimental study. *Chem. Eng. Process. - Process Intensif.* 143, 107588. <https://doi.org/10.1016/j.cep.2019.107588>
- McDonough, J.R., Ahmed, S.M.R., Phan, A.N., Harvey, A.P., 2017. A study of the flow structures generated by oscillating flows in a helical baffled tube. *Chem. Eng. Sci. J.* 171, 160–178. <https://doi.org/10.1016/j.ces.2017.05.032>
- McDonough, J.R., Oates, M.F., Law, R., Harvey, A.P., 2019b. Micromixing in oscillatory baffled flows. *Chem. Eng. J.* 361, 508–518. <https://doi.org/10.1016/j.cej.2018.12.088>
- McDonough, J.R., Phan, A.N., Harvey, A.P., 2015. Rapid process development using oscillatory baffled mesoreactors - a state-of-the-art review. *Chem. Eng. J.* 265, 110–121. <https://doi.org/10.1016/j.cej.2014.10.113>
- McGlone, T., Briggs, N.E.B., Clark, C.A., Brown, C.J., Sefcik, J., Florence, A.J., 2015. Oscillatory flow reactors (OFRs) for continuous manufacturing and crystallization. *Org. Process Res. Dev.* 19, 1186–1202. <https://doi.org/10.1021/acs.oprd.5b00225>
- McLachlan, H., Ni, X., 2016. On the effect of added impurity on crystal purity of urea in an oscillatory baffled crystallizer and a stirred tank crystallizer. *J. Cryst. Growth* 442, 81–88. <https://doi.org/10.1016/j.jcrysgro.2016.03.001>
- Mena, P.C., Pons, M.N., Teixeira, J.A., Rocha, F.A., 2005. Using image analysis in the study of multiphase gas absorption. *Chem. Eng. Sci.* 60, 5144–5150. <https://doi.org/10.1016/j.ces.2005.04.049>

- Mignard, D., Amin, L., Ni, X., 2004. Modelling of droplet breakage probabilities in an oscillatory baffled reactor. *Chem. Eng. Sci.* 59, 2189–2200. <https://doi.org/10.1016/j.ces.2004.02.012>
- Mignard, D., Amin, L.P., Ni, X., 2006. Determination of breakage rates of oil droplets in a continuous oscillatory baffled tube. *Chem. Eng. Sci.* 61, 6902–6917. <https://doi.org/10.1016/j.ces.2006.07.025>
- Mortazavi, H., Pakzad, L., 2020. The hydrodynamics and mixing performance in a moving baffle oscillatory baffled reactor through computational fluid dynamics (CFD). *Processes* 8, 1236. <https://doi.org/doi:10.3390/pr8101236>
- Muñoz-Cámara, J., Solano, J.P., Pérez-García, J., 2021. Analytical calculation of the flow superposition effect on the power consumption in oscillatory baffled reactors. *Chem. Eng. Sci.* 229, 116084. <https://doi.org/10.1016/j.ces.2020.116084>
- Muñoz-Cámara, J., Solano, J.P., Pérez-García, J., 2020. Experimental correlations for oscillatory-flow friction and heat transfer in circular tubes with tri-orifice baffles. *Int. J. Therm. Sci.* 156, 106480. <https://doi.org/10.1016/j.ijthermalsci.2020.106480>
- Muster-Slawitsch, B., Buchmaier, J., Brunner, C., Nidetzky, B., Gudimich, R.K., Harvey, A.P., Phan, A.N., 2020. Oscillating flow bioreactors : an enabling technology for sustainable biorefining operations? *J. Adv. Manuf. Process.* 2, 1–7. <https://doi.org/10.1002/amp2.10046>
- Navarro-Fuentes, F., Keane, M., Ni, X.W., 2019a. A comparative evaluation of hydrogenation of 3-butyn-2-ol over Pd/Al<sub>2</sub>O<sub>3</sub> in an oscillatory baffled reactor and a commercial parr reactor. *Org. Process Res. Dev.* 23, 38–44. <https://doi.org/10.1021/acs.oprd.8b00324>
- Navarro-Fuentes, F., Keane, M., Ni, X.W., 2019b. The effects of modes of hydrogen input and reactor configuration on reaction rate and H<sub>2</sub> efficiency in the catalytic hydrogenation of alkynol to alkenol. *Can. J. Chem. Eng.* 98, 1–8. <https://doi.org/10.1002/cjce.23615>
- Ni, X., 1995. A study of fluid dispersion in oscillatory flow through a baffled tube. *J. Chem. Technol. Biotechnol.* 64, 165–174. <https://doi.org/10.1002/jctb.280640209>
- Ni, X., Brogan, G., Struthers, A., Bennett, D.C., Wilson, S.F., 1998a. A systematic study of the effect of geometrical parameters on mixing time in oscillatory baffled columns. *Chem. Eng. Res. Des.* 76, 635–642. <https://doi.org/10.1205/026387698525162>
- Ni, X., Cosgrove, J.A., Cumming, R.H., Greated, C.A., Murray, K.R., Norman, P., 2001a. Experimental study of flocculation of bentonite and *alcaligenes eutrophus* in a batch oscillatory baffled flocculator. *Chem. Eng. Res. Des.* 79, 33–40. <https://doi.org/10.1205/026387601528507>
- Ni, X., Fitch, A.W., Jian, H., 2004a. Numerical and experimental investigations into the effect of gap between baffle and wall on mixing in an oscillatory baffled column. *Int. J. Chem. React. Eng.* 2, 1–16. <https://doi.org/https://doi.org/10.2202/1542-6580.1147>
- Ni, X., Gao, S., 1996a. Scale-up correlation for mass transfer coefficients in pulsed baffled reactors. *Chem. Eng. J. Biochem. Eng. J.* 63, 157–166. [https://doi.org/10.1016/S0923-0467\(96\)03120-X](https://doi.org/10.1016/S0923-0467(96)03120-X)
- Ni, X., Gao, S., 1996b. Mass transfer characteristics of a pilot pulsed baffled reactor. *J. Chem.*

Technol. Biotechnol. 65, 65–71. [https://doi.org/10.1002/\(SICI\)1097-4660\(199601\)65:1<65::AID-JCTB352>3.0.CO;2-1](https://doi.org/10.1002/(SICI)1097-4660(199601)65:1<65::AID-JCTB352>3.0.CO;2-1)

- Ni, X., Jian, H., Fitch, A., 2003a. Evaluation of turbulent integral length scale in an oscillatory baffled column using large eddy simulation and digital particle image velocimetry. *Chem. Eng. Res. Des.* 81, 842–853. <https://doi.org/10.1205/026387603322482086>
- Ni, X., Jian, H., Fitch, A.W., 2002. Computational fluid dynamic modelling of flow patterns in an oscillatory baffled column. *Chem. Eng. Sci.* 57, 2849–2862. [https://doi.org/10.1016/S0009-2509\(02\)00081-7](https://doi.org/10.1016/S0009-2509(02)00081-7)
- Ni, X., Johnstone, J.C., Symes, K.C., Grey, B.D., Bennett, D.C., 2001b. Suspension polymerization of acrylamide in an oscillatory baffled reactor: from drops to particles. *AIChE J.* 47, 1746–1757. <https://doi.org/10.1002/aic.690470807>
- Ni, X., Liao, A., 2008. Effects of cooling rate and solution concentration on solution crystallization of L-glutamic acid in an oscillatory baffled crystallizer. *Cryst. Growth Des.* 8, 2875–2881. <https://doi.org/10.1021/cg7012039>
- Ni, X., Mackley, M.R., Harvey, A.P., Stonestreet, P., Baird, M.H.I., Rao, N.V.R., 2003b. Mixing through oscillations and pulsations—a guide to achieving process enhancements in the chemical and process industries. *Trans IChemE* 81, 373–383. <https://doi.org/10.1205/02638760360596928>
- Ni, X., Valentine, A., Liao, A., Sermage, S.B.C., Thomson, G.B., Roberts, K.J., 2004b. On the crystal polymorphic forms of L-glutamic acid following temperature programmed crystallization in a batch oscillatory baffled crystallizer. *Cryst. Growth Des.* 4, 1129–1135. <https://doi.org/10.1021/cg0498271>
- Ni, X., Zhang, Y., Mustafa, I., 1999. Correlation of polymer particle size with droplet size in suspension polymerisation of methylmethacrylate in a batch oscillatory-baffled reactor. *Chem. Eng. Sci.* 54, 841–850. [https://doi.org/10.1016/S0009-2509\(98\)00279-6](https://doi.org/10.1016/S0009-2509(98)00279-6)
- Ni, X., Zhang, Y., Mustafa, I., 1998b. An investigation of droplet size and size distribution in methylmethacrylate suspensions in a batch oscillatory-baffled reactor. *Chem. Eng. Sci.* 53, 2903–2919.
- Nogueira, X., Taylor, B.J., Gomez, H., Colominas, I., Mackley, M.R., 2013. Experimental and computational modeling of oscillatory flow within a baffled tube containing periodic-tri-orifice baffle geometries. *Comput. Chem. Eng.* 49, 1–17. <https://doi.org/10.1016/j.compchemeng.2012.09.015>
- Oliva, J.A., Pal, K., Barton, A., Firth, P., Nagy, Z.K., 2018. Experimental investigation of the effect of scale-up on mixing efficiency in oscillatory flow baffled reactors (OFBR) using principal component based image analysis as a novel noninvasive residence time distribution measurement approach. *Chem. Eng. J.* 351, 498–505. <https://doi.org/10.1016/j.cej.2018.06.029>
- Oliveira, M.S.N., Ni, X., 2004. Effect of hydrodynamics on mass transfer in a gas-liquid oscillatory baffled column. *Chem. Eng. J.* 99, 59–68. <https://doi.org/10.1016/j.cej.2004.01.002>

- Oliveira, M.S.N., Ni, X., 2001. Gas hold-up and bubble diameters in a gassed oscillatory baffled column. *Chem. Eng. Sci.* 56, 6143–6148. [https://doi.org/10.1016/S0009-2509\(01\)00257-3](https://doi.org/10.1016/S0009-2509(01)00257-3)
- Onyemelukwe, I.I., Benyahia, B., Reis, N.M., Nagy, Z.K., Rielly, C.D., 2018. The heat transfer characteristics of a mesoscale continuous oscillatory flow crystalliser with smooth periodic constrictions. *Int. J. Heat Mass Transf.* 123, 1109–1119. <https://doi.org/10.1016/j.ijheatmasstransfer.2018.03.015>
- Palma, M., Giudici, R., 2003. Analysis of axial dispersion in an oscillatory-flow continuous reactor. *Chem. Eng. J.* 94, 189–198. [https://doi.org/10.1016/S1385-8947\(03\)00057-3](https://doi.org/10.1016/S1385-8947(03)00057-3)
- Peña, R., Oliva, J.A., Burcham, C.L., Jarmer, D.J., Nagy, Z.K., 2017. Process intensification through continuous spherical crystallization using an oscillatory flow baffled crystallizer. *Cryst. Growth Des.* 17, 4776–4784. <https://doi.org/10.1021/acs.cgd.7b00731>
- Pereira, F.M., Sousa, D.Z., Alves, M.M., Mackley, M.R., Reis, N.M., 2014. CO<sub>2</sub> dissolution and design aspects of a multiorifice oscillatory baffled column. *Ind. Eng. Chem. Res.* 53, 17303–17316. <https://doi.org/10.1021/ie403348g>
- Pereira, N.E., Ni, X., 2001. Droplet size distribution in a continuous oscillatory baffled reactor. *Chem. Eng. Sci.* 56, 735–739. [https://doi.org/https://doi.org/10.1016/S0009-2509\(00\)00283-9](https://doi.org/https://doi.org/10.1016/S0009-2509(00)00283-9)
- Phan, A.N., Harvey, A.P., 2011a. Characterisation of mesoscale oscillatory helical baffled reactor - experimental approach. *Chem. Eng. J.* 180, 229–236. <https://doi.org/10.1016/j.cej.2011.11.018>
- Phan, A.N., Harvey, A.P., 2011b. Effect of geometrical parameters on fluid mixing in novel mesoscale oscillatory helical baffled designs. *Chem. Eng. J.* 169, 339–347. <https://doi.org/10.1016/j.cej.2011.03.026>
- Phan, A.N., Harvey, A.P., 2010. Development and evaluation of novel designs of continuous mesoscale oscillatory baffled reactors. *Chem. Eng. J.* 159, 212–219. <https://doi.org/10.1016/j.cej.2010.02.059>
- Phan, A.N., Harvey, A.P., Eze, V., 2012. Rapid production of biodiesel in mesoscale oscillatory baffled reactors. *Chem. Eng. Technol.* 35, 1214–1220. <https://doi.org/10.1002/ceat.201200031>
- Phan, A.N., Harvey, A.P., Lavender, J., 2011a. Characterisation of fluid mixing in novel designs of mesoscale oscillatory baffled reactors operating at low flow rates (0.3-0.6ml/min). *Chem. Eng. Process. Process Intensif.* 50, 254–263. <https://doi.org/10.1016/j.cep.2011.02.004>
- Phan, A.N., Harvey, A.P., Rawcliffe, M., 2011b. Continuous screening of base-catalysed biodiesel production using new designs of mesoscale oscillatory baffled reactors. *Fuel Process. Technol.* 92, 1560–1567. <https://doi.org/10.1016/j.fuproc.2011.03.022>
- Rasdi, F.R.M., Phan, A.N., Harvey, A.P., 2013. Rapid determination of reaction order and rate constants of an imine synthesis reaction using a mesoscale oscillatory baffled reactor. *Chem. Eng. J.* 222, 282–291. <https://doi.org/10.1016/j.cej.2013.02.080>
- Raval, V., Siddique, H., Brown, C.J., Florence, A.J., 2020. Development and characterisation of a cascade of moving baffle oscillatory crystallisers (CMBOC). *CrystEngComm* 22, 2288–2296.



<https://doi.org/10.1039/d0ce00069h>

- Reis, N., Gonçalves, C.N., Aguedo, M., Gomes, N., Teixeira, J.A., Vicente, A.A., 2006a. Application of a novel oscillatory flow micro-bioreactor to the production of  $\gamma$ -decalactone in a two immiscible liquid phase medium. *Biotechnol. Lett.* 28, 485–490. <https://doi.org/10.1007/s10529-006-0003-x>
- Reis, N., Gonçalves, C.N., Vicente, A.A., Teixeira, J.A., 2006b. Proof-of-concept of a novel micro-bioreactor for fast development of industrial bioprocesses. *Biotechnol. Bioeng.* 95, 744–753. <https://doi.org/10.1002/bit.21035>
- Reis, N., Harvey, A.P., Mackley, M.R., Vicente, A.A., Teixeira, J.A., 2005. Fluid mechanics and design aspects of a novel oscillatory flow screening mesoreactor. *Chem. Eng. Res. Des.* 83(A4), 357–371. <https://doi.org/10.1205/cherd.03401>
- Reis, N., Mena, P.C., Vicente, A.A., Teixeira, J.A., Rocha, F.A., 2007. The intensification of gas-liquid flows with a periodic, constricted oscillatory-meso tube. *Chem. Eng. Sci.* 62, 7454–7462. <https://doi.org/10.1016/j.ces.2007.09.018>
- Reis, N., Vicente, A.A., Teixeira, J.A., 2010. Liquid backmixing in oscillatory flow through a periodically constricted meso-tube. *Chem. Eng. Process. Process Intensif.* 49, 792–802. <https://doi.org/10.1016/j.cep.2010.01.014>
- Reis, N., Vicente, A.A., Teixeira, J.A., Mackley, M.R., 2004. Residence times and mixing of a novel continuous oscillatory flow screening reactor. *Chem. Eng. Sci.* 59, 4967–4974. <https://doi.org/10.1016/j.ces.2004.09.013>
- Sarkar, S., Singh, K.K., Shenoy, K.T., 2020. CFD modelling of oscillatory flow in columns having different types of internals. *Chem. Eng. Process. - Process Intensif.* 155, 108052. <https://doi.org/10.1016/j.cep.2020.108052>
- Schaber, S.D., Gerogiorgis, D.I., Ramachandran, R., Evans, J.M.B., Barton, P.I., Trout, B.L., 2011. Economic analysis of integrated continuous and batch pharmaceutical manufacturing: a case study. *Ind. Eng. Chem. Res.* <https://doi.org/10.1021/ie2006752>
- Siddique, H., Brown, C.J., Houson, I., Florence, A.J., 2015. Establishment of a continuous sonocrystallization process for lactose in an oscillatory baffled crystallizer. *Org. Process Res. Dev.* 19, 1871–1881. <https://doi.org/10.1021/acs.oprd.5b00127>
- Singh, B., Rizvi, S.S.H., 1994. Design and economic analysis for continuous countercurrent processing of milk fat with supercritical carbon dioxide. *J. Dairy Sci.* 77, 1731–1745. [https://doi.org/10.3168/jds.S0022-0302\(94\)77114-9](https://doi.org/10.3168/jds.S0022-0302(94)77114-9)
- Slavnić, D., Bugarski, B., Nikačević, N., 2019. Solids flow pattern in continuous oscillatory baffled reactor. *Chem. Eng. Process. - Process Intensif.* 135, 108–119. <https://doi.org/10.1016/j.cep.2018.11.017>
- Slavnić, D.S., Živković, L. V., Bjelić, A. V., Bugarski, B.M., Nikačević, N.M., 2017. Residence time distribution and Peclet number correlation for continuous oscillatory flow reactors. *J. Chem. Technol. Biotechnol.* 92, 2178–2188. <https://doi.org/10.1002/jctb.5242>

- Smith, K.B., 1999. The scale-up of oscillatory flow mixing. PhD Diss. Christ's Coll. Univ. Cambridge.
- Smith, K.B., Mackley, M.R., 2006. An experimental investigation into the scale-up of oscillatory flow mixing in baffled tubes. *Chem. Eng. Res. Des.* 84, 1001–1011. <https://doi.org/10.1205/cherd.05054>
- Solano, J.P., Herrero, R., Espín, S., Phan, A.N., Harvey, A.P., 2012. Numerical study of the flow pattern and heat transfer enhancement in oscillatory baffled reactors with helical coil inserts. *Chem. Eng. Res. Des.* 90, 732–742. <https://doi.org/10.1016/j.cherd.2012.03.017>
- Soufi, M.D., Ghobadian, B., Najafi, G., Mousavi, S.M., Aubin, J., 2017. Optimization of methyl ester production from waste cooking oil in a batch tri-orifice oscillatory baffled reactor. *Fuel Process. Technol.* 167, 641–647. <https://doi.org/10.1016/j.fuproc.2017.07.030>
- Stephens, G.G., Mackley, M.R., 2002. Heat transfer performance for batch oscillatory flow mixing. *Exp. Therm. Fluid Sci.* 25, 583–594. [https://doi.org/10.1016/S0894-1777\(01\)00098-X](https://doi.org/10.1016/S0894-1777(01)00098-X)
- Stonestreet, P., Harvey, A.P., 2002. A mixing-based design methodology for continuous oscillatory flow reactors. *Chem. Eng. Res. Des.* 80, 31–44. <https://doi.org/10.1205/026387602753393204>
- Stonestreet, P., Van Der Veeken, P.M.J., 1999. The effects of oscillatory flow and bulk flow components on residence time distribution in baffled tube reactors. *Chem. Eng. Res. Des.* 77, 671–684. <https://doi.org/10.1205/026387699526809>
- Sutherland, K., Pakzad, L., Fatehi, P., 2021. Mixing time and scale-up investigation of a moving-baffle oscillatory baffled column. *Chem. Eng. Technol.* 44, 1–10. <https://doi.org/10.1002/ceat.202000262>
- Sutherland, K., Pakzad, L., Fatehi, P., 2020. Oscillatory power number, power density model, and effect of restriction size for a moving-baffle oscillatory baffled column using CFD modelling. *Can. J. Chem. Eng.* 98, 1172–1190. <https://doi.org/10.1002/cjce.23713>
- Takriff, M.S., Masngut, N., Kadhum, A.A.H., Kalil, M.S., Mohammad, A.W., 2009. Solvent fermentation from palm oil mill effluent using *Clostridium acetobutylicum* in oscillatory flow bioreactor. *Sains Malaysiana* 38, 191–196.
- van Delden, M.L., Vos, G.S., Kuipers, N.J.M., de Haan, A.B., 2006. Extraction of caprolactam with toluene in a pulsed disc and doughnut column - Part II: experimental evaluation of the hydraulic characteristics. *Solvent Extr. Ion Exch.* 24, 519–538. <https://doi.org/10.1080/07366290600760649>
- Womersley, J.R., 1955. Method for the calculation of velocity, rate of flow and viscous drag in arteries when the pressure gradient is known. *J. Physiol.* 127, 553–563. <https://doi.org/10.1113/jphysiol.1955.sp005276>
- Yang, H., Yu, X., Raval, V., Makkawi, Y., Florence, A., 2015. Effect of oscillatory flow on nucleation kinetics of butyl paraben. *Cryst. Growth Des.* 16, 875–886. <https://doi.org/10.1021/acs.cgd.5b01437>

- Yoshida, J.I., Kim, H., Nagaki, A., 2011. Green and sustainable chemical synthesis using flow microreactors. *ChemSusChem* 4, 331–340. <https://doi.org/10.1002/cssc.201000271>
- Yu, Z., Lv, Y., Yu, C., 2012. A continuous kilogram-scale process for the manufacture of o-difluorobenzene. *Org. Process Res. Dev.* 16, 1669–1672. <https://doi.org/10.1021/op300127x>
- Yussof, H.W., Bahri, S.S., Mazlan, N.A., 2018. Evaluation of power density on the bioethanol production using mesoscale oscillatory baffled reactor and stirred tank reactor. *IOP Conf. Ser. Mater. Sci. Eng.* 334, 012070. <https://doi.org/10.1088/1757-899X/334/1/012070>
- Zhao, L., Raval, V., Briggs, N.E.B., Bhardwaj, R.M., McGlone, T., Oswald, I.D.H., Florence, A.J., 2014. From discovery to scale-up:  $\alpha$ -lipoic acid: nicotinamide co-crystals in a continuous oscillatory baffled crystalliser. *CrystEngComm* 16, 5769–5780. <https://doi.org/10.1039/c4ce00154k>
- Zheng, H., Yan, Z., Chu, S., Chen, J., 2018. Continuous synthesis of isobornyl acetate catalyzed by a strong acid cation exchange resin in an oscillatory flow reactor. *Chem. Eng. Process. - Process Intensif.* 134, 1–8. <https://doi.org/10.1016/j.cep.2018.10.005>